Journal of ELECTRONIC MATERIALS, Vol. 47, No. 2, 2018
DOI: 10.1007/s11664-017-5876-z

Effects of Various Parameters on Structural and Optical Properties of CBD-Grown ZnS Thin Films: A Review

TARKESHWAR SINHA,[1] DEVJYOTI LILHARE,[1] and AYUSH KHARE[1,2]

1.—Department of Physics, National Institute of Technology, Raipur 492010, India. 2.—e-mail: akhare.phy@nitrr.ac.in

Zinc sulfide (ZnS) thin films deposited by chemical bath deposition (CBD) technique have proved their capability in a wide area of applications including electroluminescent and display devices, solar cells, sensors, and field emitters. These semiconducting thin films have attracted a much attention from the scientific community for industrial and research purposes. In this article, we provide a comprehensive review on the effect of various parameters on various properties of CBD-grown ZnS films. In the first part, we discuss the historical background of ZnS, its basic properties, and the advantages of the CBD technique. Detailed discussions on the film growth, structural and optical properties of ZnS thin films affected by various parameters, such as bath temperature and concentration, deposition time, stirring speed, complexing agents, pH value, humidity in the environment, and annealing conditions, are also presented. In later sections, brief information about the recent studies and findings is also added to explore the scope of research work in this field.

Key words: ZnS, chemical bath deposition, film growth, CIGS solar cell, thin films

INTRODUCTION

ZnS is a very promising direct band-gap semiconductor that has proved its capability in various fields including solar cells, flat panel displays, field emitters, lasers, photonics, electronics, sensing, and catalysis.[1–3] In 1603, an Italian alchemist Vincenzo Cacariolo was trying to make gold using $BaSO_4$. Obviously, he did not obtain gold, but, unknowingly, he discovered a material that was going to be the part of one of the most studied fields in research.[4] At that time, nobody knew how light emission occurred, but unintentionally that alchemist found a luminescent host, barium sulfide.[5] In the next three centuries, three luminescent phosphors were synthesized. In 1700, Friedrich Hoffmann prepared calcium sulfide, in 1817, J.F. John synthesized strontium sulfide, and, in 1866, one of the most frequently used phosphors of the twentieth century, zinc sulfide (ZnS) was synthesized by Theodor Sidot.[6] For ZnS, the first remarkable breakthrough was obtained by Destriau in 1936, when he applied a very high voltage in his experiment in which ZnS powder was suspended in insulating castor oil, and it was separated from other electrodes by a mica sheet.[7] After Destriau's experiment, ZnS remained one of the most preferred electroluminescent (EL) materials for several decades.

ZnS is a flexible material and available in different dimensions ranging from 0D to 3D,[8–10] and in size and shape including spherical, wire, ribbon, rod-like, tube-like, and thin and thick film form.[11–14] These variations in the features of ZnS have helped it to be used in various sectors such as electronic and optoelectronic devices as well as health and safety devices.[15–21] In general, the blue color response has been detected in the lower wavelength region of ZnS. In order to activate the longer wavelength region, many researchers have successfully replaced Zn by some popular transition metal ions, such as Sn, Ni, Cd, Fe, Mn, and Cu.[22–24]

In recent times, nanostructured materials, including ZnS, ZnO, and cadmium sulfide (CdS),

(Received July 31, 2017; accepted October 10, 2017; published online October 27, 2017)

have become one of the most preferable research branches, which is gradually increasing its role in daily life.[25–28] ZnS exhibits some special properties due to which it has become a sufficiently tough competitor of the widely studied nanostructured material, zinc oxide (ZnO). For example, its energy band-gap ($\sim$ 3.7 eV) is wider than that of ZnO ($\sim$ 3.4 eV). When thin film solar cell technology was explored, ZnS also proved its importance in the form of semiconducting thin films. While manufacturing a good-quality copper indium gallium diselenide (CIGS) solar cell, scientists faced problems to obtain the film of a sufficiently large area and to find more environmentally friendly substitutes as compared to previously encountered materials. In the case of CIGS solar cells, a remarkable conversion efficiency of 22.8% has recently been achieved.[29] CdS has been found to be a superior and dominating semiconducting buffer layer of CIGS solar cells compared with all its nearest competitors. However, it is very toxic in nature and responds badly towards incident radiations of shorter wavelengths. Also, CdS might be a reason behind any reduction in quantum efficiency of the device due to its smaller energy band-gap of 2.4 eV, which opposes the transmission of light of wavelength less than 500 nm to the absorbing layer.[30,31]

Some researchers have replaced the CdS buffer layer by a ZnS buffer layer and have reported an efficient solar cell with an eco-friendly character and good absorbing behavior towards the shorter wavelength light due to its larger band-gap.[32–34] When CBD–ZnS film was used as a buffer layer in CIGS solar cells, the device offered an efficiency of almost 18.6%, proving its reliability to become a suitable replacement for CdS.[35]

In this article, we provide a comprehensive review of various properties of ZnS thin films deposited by the CBD technique. We begin with some historical milestones in the investigation towards ZnS material followed by its basic properties. Subsequently, we discuss the benefits of the CBD technique for ZnS thin films preparation and observed variations in its properties like film growth rate, crystalline nature, surface morphology, and optical spectra.

BASIC PROPERTIES OF ZnS

ZnS is a II–VI group semiconducting material. If the transition from the valence band to the conduction band is taken into account, the momentum is found to be conserved,[36,37] indicating that ZnS is a direct band-gap semiconductor. The plots between photon energy ($h\upsilon$) and $(\alpha h\upsilon)^2$ are found to be linear at the absorption edge, which is further evidence for the direct band-gap nature of ZnS. ZnS is commonly obtained in two crystalline forms: (1) cubic or zinc blende (ZB) structure and (2) hexagonal or wurtzite (WZ) structure. Researchers can work with ZnS at sufficiently high enough temperatures due to its high melting point (1800–1900°C). The lattice parameters of ZnS related to the cubic and hexagonal phases are obtained with a tiny, but recognizable, margin. For the ZB structure, $a = b = c = 5.41$ Å with $Z = 4$, and for the WZ phase, $a = b = 3.82$ Å, $c = 6.26$ Å with $Z = 2$. This slight variation in the atomic arrangement creates a recognizable difference in the physical properties of these two phases.[38] The observed band-gap for the ZB structure is 3.72 eV,[39] and for WZ it is 3.77 eV.[40] These distinct phases are formed at different temperatures. The cubic phase is a low-temperature phase, while the hexagonal phase is a high-temperature polymorph. Figure 1 presents the visual distinction between the WZ and ZB structures of ZnS. From Fig. 1, it can be easily seen that the zinc and sulfur ions arrange themselves in an ordered pattern, as ABABAB for the WZ phase and the ABCABC pattern for the ZB phase.

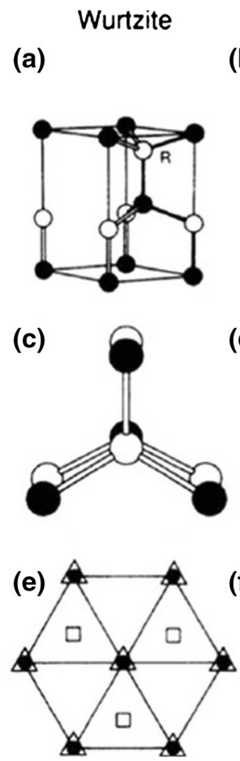

Fig. 1. Models showing the difference between wurtzite and zinc blend crystal structures. (a, b) The handedness of the fourth interatomic bond along the right (*R*) for wurtzite and along the left (*L*) for zinc blend. (c, d) The respective eclipsed and staggered dihedral conformations. (e, f) The atomic arrangement along the close packing axis. Reprinted with permission from Ref. 38.

SYNTHESIS TECHNIQUE: CHEMICAL BATH DEPOSITION

A collection of deposition techniques are available these days to deposit ZnS thin films. They can be categorized into two different classes. The first group are the physical deposition techniques, which include thermal evaporation (TE), sputtering, molecular beam epitaxy, and ion plotting.[41,42] The

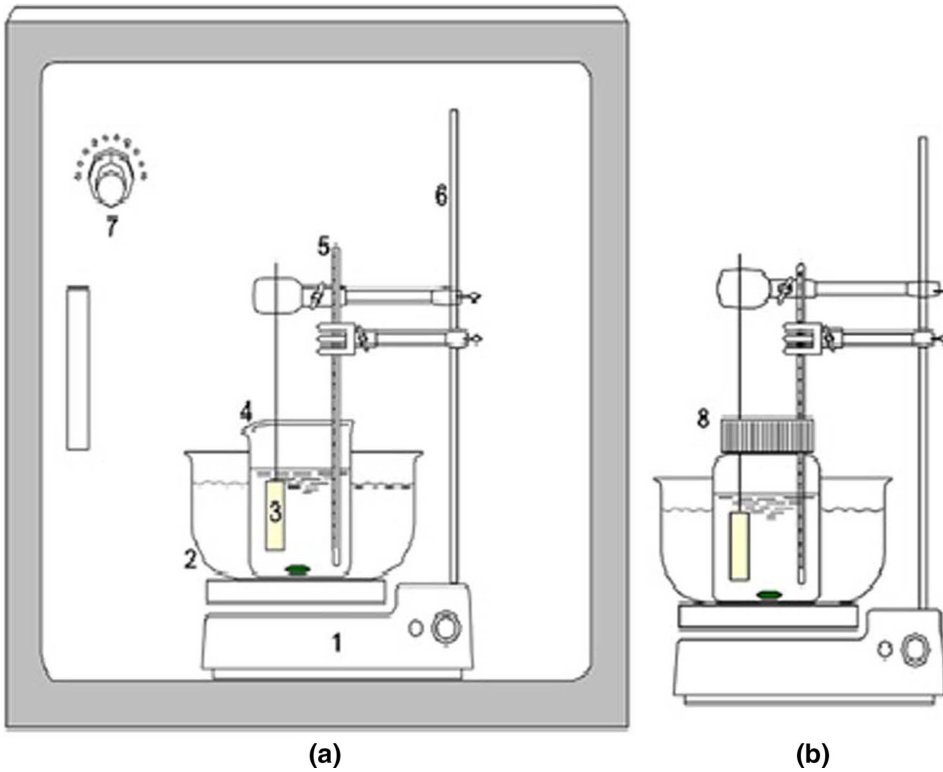

Fig. 2. The experimental set-up for chemical bath deposition by the open (a) and the hermetic system (b); 1 magnetic stirrer, 2 bowl bath, 3 sample substrate, 4 beaker, 5 thermometer, 6 clamp stand, 7 humidity controller, 8 capped wide-necked bottle. Reprinted with permission from Elsevier from Ref. 71.

second class of deposition techniques is of chemical deposition techniques in which the deposition process depends mainly on the chemical reactions. Some of the well-known chemical deposition techniques are chemical vapor deposition, chemical bath deposition (CBD), spray pyrolysis, and electrochemical deposition.[43] Most of the physical deposition techniques provide thin films of better quality than that of a chemical one, but they demand high energy with a high-quality target in vacuum. On the other hand, chemical techniques require a simple and easy experimental set-up including fewer instruments and have the potential to produce thin films on larger areas. In our opinion, the most important thing is what there is in the laboratory. Since it is not possible to have sophisticated instruments everywhere, one must try to fully utilize the existing set-up and optimize what you have.

In this review, we restrict our discussion on the deposition of ZnS films mainly by the CBD technique. CBD yields stable, adherent, uniform and hard films with good reproducibility by a relatively simple process. CBD requires a small and portable apparatus. For the sake of preparing an impurity-free sample, a closed and isolated apparatus is desirable.

Synthesis of ZnS film by CBD commonly refers to the main reaction between Zn^{2+} and S^{2-} ions, and thus it belongs to the one-pot synthesis method. In this method, a solution of a Zn-based precursor, generally zinc acetate [$Zn(CH_3COO)_2$], zinc sulfate ($ZnSO_4$), or zinc chloride ($ZnCl_2$) and a sulfur-based reagent commonly thiourea [$CS(NH_2)_2$] are mixed. In addition, one or more complexing agents such as ammonia solution (NH_4OH), tri-sodium citrate (TSC) ($Na_3C_6H_5O_7$), triethanolamine (TEA) ($C_6H_{15}NO_3$), Na_2-EDTA ($Na_2C_{10}H_{16}N_2O_8$) or hydrazine hydrate (HH) (N_2H_4) that play an additional role in maintaining a constant pH value are also introduced into the solution. The purity of chemicals is another fundamental concern for all who wish to carry out good research as it may have a considerable effect on the results. The main feature of CBD is that the reaction commences only when the solution, with the substrate dipped inside, is placed in a bath maintained within a suitable temperature range depending on the demand of material formation. Below this temperature or at room temperature (RT), it is very difficult to deposit a ZnS film via CBD. A water bath is used for deposition in the CBD process. In this equipment, a container is filled with heated water and a sample is placed in the water bath at a constant temperature over a certain period of time. In CBD, the structural and optical properties can be controlled by changing the bath temperature, solution pH, stirring speed, reagent concentration, complexing agent, deposition time, and annealing conditions. The effects of these

Table I. Details of recent investigations on preparative conditions and properties of CBD-ZnS films

Study no.	Bath composition	pH value	Film thickness (nm)	Deposition temperature (°C)	Deposition time	Substrate	Remarks	Reference
1	$ZnCl_2$, $SC(NH_2)_2$, NH_3, N_2H_4	10–11.5	–	90	3 h	Glass	Transmittance = 70% and E_g = 3.67 eV[a]	66
2	$Zn(CH_3COO)_2{\cdot}2H_2O$, $SC(NH_2)_2$, $C_4H_6O_6$, $N_2H_4{\cdot}H_2O$, NH_3	10	50–110	85	3 h	Glass	Transmittance = 80–100% and E_g = 3.69 eV[b]	72
3	$ZnCl_2$, $SC(NH_2)_2$, NH_3, $N_2H_4{\cdot}H_2O$	10–11.5	–	90	3 h	SnO_2 coated glass	Transmittance = 70%[c]	92
4	$ZnSO_4$, $SC(NH_2)_2$, NH_3	–	120–140	80, 90	20–80 min	Glass	Transmittance > 90% and E_g = 3.51 eV[d]	73
5	$ZnSO_4$, $SC(NH_2)_2$, NH_3	–	–	81	40 and 60 min	Glass	Transmittance = 70–88% and E_g = 3.63 eV[e]	60
6	$Zn(CH_3COO)_2.2H_2O$, C_2H_5NS, $Na_2C_{10}H_{16}N_2O_8$, $C_6H_{12}N_4$	10	37–135	80	2 h	Glass	Transmittance = 70–80%, E_g = 3.75–3.87 eV[f]	95
7	$Zn(CH_3COO)_2{\cdot}2H_2O$, $SC(NH_2)_2$, $Na_2C_{10}H_{16}N_2O_8$, $Na_3C_6H_5O_7$, NH_4OH	10	100	80	4 h	ITO coated glass	Transmittance = 60–70%, grain size = 30–100 nm, and E_g = 3.5–3.89 eV[g]	76
8	$Zn(CH_3COO)_2{\cdot}2H_2O$, $SC(NH_2)_2$, NH_4OH, Na_3-$C_6H_5O_7$, $C_{10}H_{16}N_2O_8$	10	Without complexing agent 50, With TSC 110, with TSC and EDTA 130	80	4 h	Glass	Transmittance = 85, 65, and 70%, grain size = 30–100 nm, and E_g = 3.94 eV, 3.87 eV, and 3.84 eV[h]	62
9	$Zn(CH_3COO)_2.2H_2O$, $SC(NH_2)_2$ $Na_3C_6H_5O_7$, NH_4OH	10	70–140	80	4 h	Glass	Transmittance = 75–85% and energy band–gap E_g = 3.73–3.80 eV[i]	63
11	$ZnSO_4$, $SC(NH_2)_2$, $N_2H_4{\cdot}H_2O$, NH_4OH	–	80	70	2 h	Soda lime glass	Transmittance > 70%, E_g = 3.76–3.87 eV[k]	93
12	$ZnCl_2$, $ZnSO_4.7H_2O$, $Zn(NO_3)_2.6H_2O$, $Zn(CH_3COO)_2.2H_2O$, CH_4N_2O, C_2H_5NS	5.9–6.1	140–175	85	4 h	Glass	Particle size = 12.5–15.5 nm and E_g = 3.66–3.83 eV[l]	77
13	$ZnSO_4$. $7H_2O$, $SC(NH_2)_2$, NH_4OH, $N_2H_4{\cdot}H_2O$	–	–	50 –90	1.5–2.5 h	Soda lime glass	Transmittance = 90%, E_g = 3.93–4.06 eV[m]	55
14	$ZnSO_4.7H_2O$, $CS(NH_2)_2$, NH_4OH, $N_2H_4{\cdot}H_2O$	9–11	54–122	80	1 h	Glass	Transmittance = 75% to 80% and E_g = 4.0–4.2 eV[n]	68
15	$ZnSO_4{\cdot}7H_2O$, $SC(NH_2)_2$, $N_2H_4{\cdot}H_2O$, NH_4OH	9.7	90–110	80	20–120 min	Glass	Transmittance = 77% and E_g = 3.76–3.98 eV[o]	71
16	$Zn(CH_3COO)_2{\cdot}2H_2O$, $CS(NH_2)_2$, $N_2H_4O_3$, $N_2H_4{\cdot}H_2O$, $Na_3C_6H_5O_7$, $C_6H_{15}NO_3$	10	HH 560 TEA 740 TSC 860	80	2 h	Glass	Transmittance = 50–87% and E_g = 3.57–3.73 eV[p]	64
17	$ZnSO_4{\cdot}7H_2O$, $CS(NH_2)_2$, $Na_3C_6H_5O_7$, $C_4H_6O_6$, KOH	10.5	–	75	4–16 h	Soda lime glass	Transmittance = 80% and E_g = 3.71–3.83 eV[q]	96

Table I. continued

Study no.	Bath composition	pH value	Film thickness (nm)	Deposition temperature (°C)	Deposition time	Substrate	Remarks	Reference
18	$ZnSO_4 \cdot 7H_2O$, $SC(NH_2)_2$, NH_4OH	–	–	Step 1 80 Step 2 60 80	40 min 10 min 40 min	Bare and ITO glass	Transmittance = 30–80%, E_g = 3.67–3.68 eV (bare glass) and E_g = 3.62–3.65 eV (ITO glass)[r]	94
19	$Zn(CH_3COO)_2 \cdot 2H_2O$, $Na_2C_{10}H_{16}N_2O_8$, C_2H_5NS	4	120–610	95	2–6 h	Glass	Transmittance = 60–83%[s]	81

[a]The crystalline behavior was compromised when the pH value exceeded the higher side of the range 10–11.5. Optical transmittance was increased and band-gap was decreased due to increment in pH value.[b]CBD ZnS film became thicker with the increment in deposition temperature. Wurtzite-structured ZnS film was obtained. Annealing at 500°C helped to improve the crystallinity and smoothness of the surface of the film with a grain size < 100 nm.[c]A closely packed and uniform film is deposited by a cluster growth mechanism. A decrement in pH value from 11.5 to 10 resulted in the improvement in the crystalline nature of the film. A β-ZnS peak is also introduced along with cubic (111) phase.[d]The film had a cubic structure with amorphous $Zn(OH)_2$, and cubic ZnS and ZnO peak were obtained after annealing at 200°C.[e]Stirring speed affected the thickness of the film only for a homogeneous process, not a heterogeneous process. For longer deposition times, the thickness of the film was increased by increasing the speed of stirring.[f]Films deposited using hexamethylenetetramine (HMTA) as a complexing agent showed a uniform but rough morphology as compared to other films prepared using Na_2-EDTA. Film growth was increased by increasing the concentration of HMTA. Deposited films had cubic (111) and hexagonal (006) phases.[g]The best crystalline film was obtained after annealing at 500°C in a N_2 + H_2S atmosphere and the rest of the deposited films were poorly crystallized. The film showed a drop in the transmittance in the visible region after annealing treatment.[h]The film deposited without any complexing agent was poorly crystallized. After introducing complexing agents to the solution, a crystalline structure with a (111) peak was obtained and the surface of the film became uniform, smooth and closely packed with particles having grain size 30–100 nm. Complexing agents helped to increase the thickness of the films.[i]The thickness of the deposited film was decreased due to the increase in the concentration of TSC. Optical transmittance in the visible region was around 75% and 85% with 0 M and 0.2 M TSC, respectively. The crystalline nature was slightly improved with the increasing concentration of TSC.[j]The thickness of film varied irregularly upon increasing the deposition temperature, and ,after annealing treatment, the thickness was observed to change. Optical transmittance also decreased by annealing due to compactness and removal of space between the particles. It was more than 75% for wavelengths larger than 600 nm. The films were poorly crystalline or amorphous in nature as none of the characteristic peaks were obtained in the XRD patterns. The EDS analysis proved the presence of Zn and S particles.[k]For lower NH_3/N_2H_4 ratios, film growth was dominated by the cluster-by-cluster mechanism. For higher NH_3/N_2H_4, film growth was dominated by the ion-by-ion mechanism. The surface morphology became homogeneous and dense upon increasing the concentrations of thiourea and ammonia.[l]Four different zinc salts were used to deposit ZnS films in order to find the best precursor material to deposit ZnS films by CBD. Films prepared using $ZnCl_2$ had better crystallinity and morphology. It was concluded that $ZnCl_2$ was the best Zn-source material for CBD–ZnS films.[m]The thickness and optical transmittance increased with increasing deposition temperature. pH value decreased due to the increment in temperature. Films showed a cubic crystalline nature.[n]The growth rate was affected by varying pH value of the solution. As-deposited films were almost amorphous in nature, and annealing of films (prepared at higher pH values) at 550°C helped to improve the crystalline structure.[o]Effects of humidity on the properties of ZnS thin film were investigated in both open and closed systems. RH values were 60%, 70% and 80%. All films were poorly crystalline. Relative humidity in the environment was responsible for the decrement in transmittance in the visible region. At RH 70%, a uniform film was obtained and for rest of two RH values films had a powdery surface.[p]The film deposited using HH-ammonia solution as a complexing agent was more uniform and smoother than that of the films deposited by using other agents. The observed band-gap value of this film was 3.73 eV with 87% transmittance in the visible region. Two other two films with TEA-TSC and TSC-ammonia showed medium and low transmittance due to higher thickness, but they exhibited excellent luminescent properties and their band-gap was lower than the previous one.[q]Non-toxic complexing agents were used to prepare ZnS thin films. The transmittance (almost 80%) was thickness-dependent. The hexagonal phase was identified in the XRD pattern. The particle size and band-gap were found to decrease with increasing deposition time.[r]The film showed high transmittance and low absorbance with the shifting of the wavelength towards a higher range, i.e., more than 700 nm. A cubic structure with β-ZnS phase was obtained. The surface of the film was very smooth and particles covered it densely. The crystalline size in the case of the film on ITO-coated glass was more than that of the film on bare glass, and grain size increased upon annealing of film. The authors found that the optical, structural or morphological properties of the CBD-ZnS film were independent of the substrate.[s]In XRD patterns, a hexagonal WZ phase was obtained and the intensity of peaks increased upon increasing the deposition time beyond 3 h. Surface morphology, optical spectra, and band-gap values were found to change in a linear fashion for 2-h- to 5-h-deposited samples, but for the deposition time of 6 h, they changed abruptly.

parameters will be discussed in detail in subsequent sections.

In the past, the CBD method has been used to prepare many chalcogenides, ternary, quaternary, penternary, and chalcopyrite materials including CdS, ZnSe, ZnO, CdTe, and $CuInS_2$. Most researchers in this area were inspired and illustrated by the work of Refs. 44, 45, and 46 and others. In the last decades of the twentieth century, the CBD technique also established itself in the field of solar energy applications. An large number of papers reporting progress on CBD grown films are published every year.

In 1989, the application of CBD for solar control coatings was suggested by Ref. 47. The following year, CBD was used for the synthesis of different layers in a solar cell and gave an appreciable efficiency of 11%.[48] This marked the beginning of a new era in which CBD opened new avenues for solar cell-related research. Figure 2 shows a typical experimental set-up used for CBD. A water bath is needed for placing the solution with a substrate dipped inside, and a magnetic stirrer to mix the chemicals thoroughly in the solution. Very expensive materials subjected to high purity are not essential for CBD which establishes it as a less costly technique. Employing CBD for deposition of different materials also depends on their nature. More care needs to be taken while working with toxic materials like CdS, PbS, and CdTe. Although CBD is a less hazardous process to some extent, for the sake of safety, it is suggested that researchers should use a fume hood and deposit films using non-toxic complexing agents.

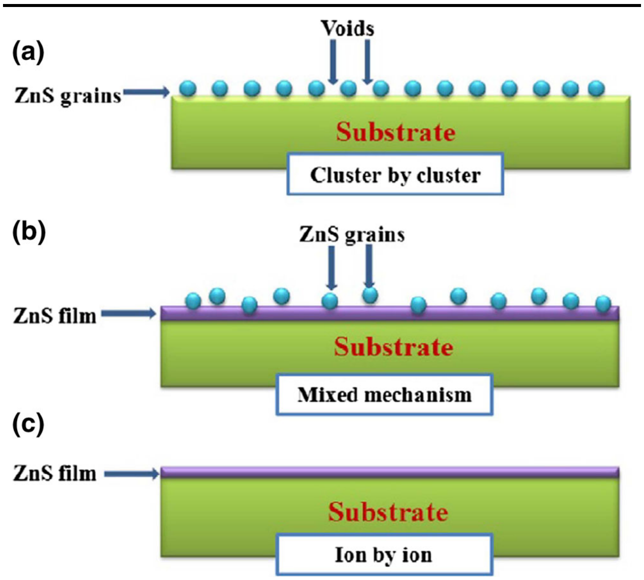

Fig. 3. Schematic illustrations to describe the formation of ZnS thin film (a) cluster by cluster growth (b) mixed growth (cluster by cluster and ion by ion) (c) ion by ion growth. Reprinted with permission from Elsevier from Ref. 63.

For commercial purposes, a large area deposition is required, which can also be achieved by CBD. Depending upon the volume of solution, size of the substrate, and shape of the holder, a desired experimental set-up can be designed and an appreciable large area of the substrate can be deposited in the form of thin or thick films. During the journey, from the beginning to the present days, CBD has emerged as one of the popular techniques to produce large area thin films for solar cells and for other applications.

RECENT INVESTIGATIONS

The following sections review the study of variations in different properties of CBD–ZnS thin films due to different preparative conditions. In recent times, many researchers deposited ZnS films by CBD and explained the experimental outcomes. Table I provides concise information about the experiments performed to investigate various properties of ZnS thin films in the last few years.

REACTION MECHANISM

In order to deposit a semiconductor film through CBD, generally, a soda-lime, fluorine tin oxide- (FTO) or indium tin oxide- (ITO) coated glass is preferred. A solution containing cation and anion sources with one or more chelating agent needs to be prepared. One of the limitations associated with the deposition of ZnS thin films by the CBD technique is that the growth rate is low, and is almost 70 nm/h,[49] whereas some other deposition techniques such as TE and photochemical deposition provide a huge growth rate of $\sim 1\ \mu$m/h. However, this limitation becomes CBD's major advantage for solar cell application in which

Table II. Thickness of the deposited and annealed ZnS thin films

Deposition temperature (°C)	Thickness of as-deposited film (nm)	Thickness of film after annealing (nm)
75	79	73
80	102	145
85	155	111
90	119	200
95	96	156

Reprinted permission from Elsevier from Ref. 54.

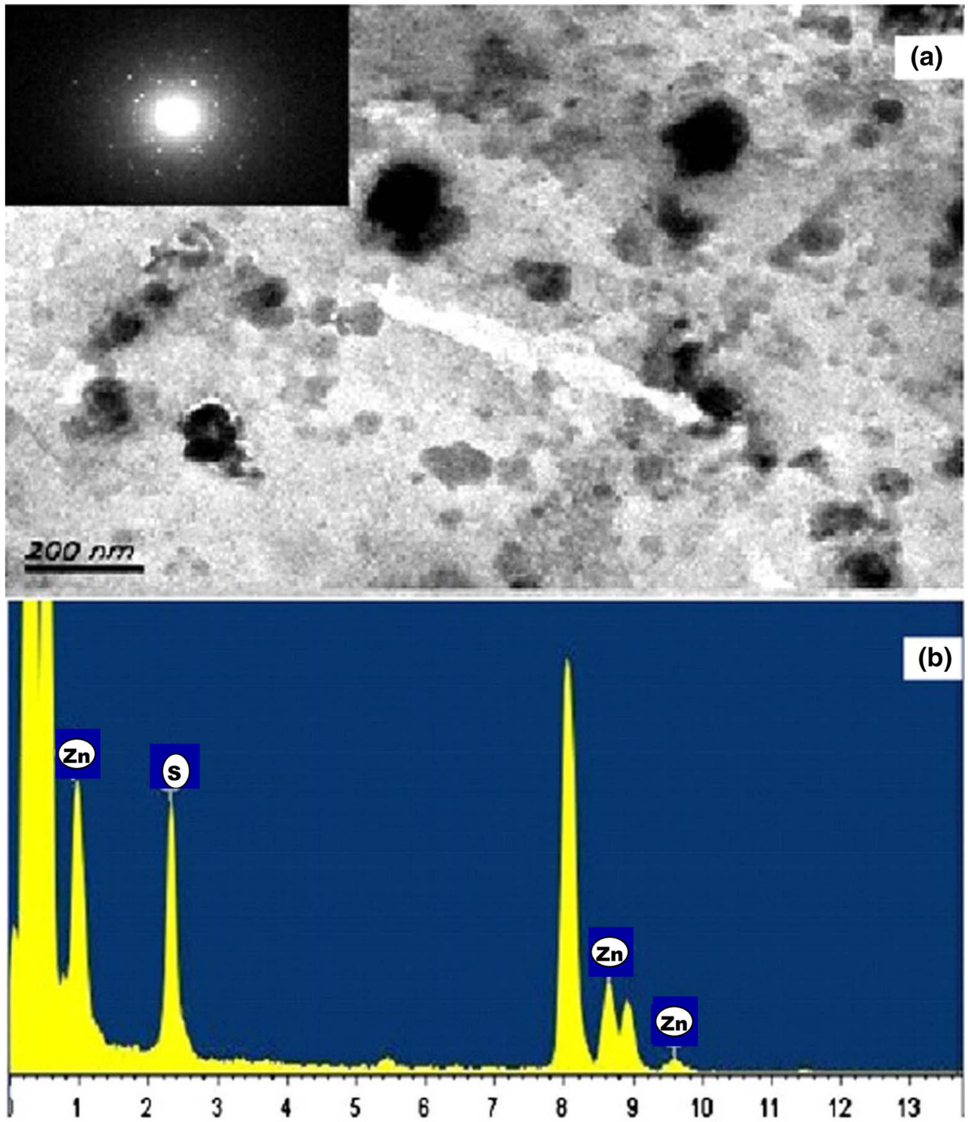

Fig. 4. TEM image, electron diffraction pattern (insets) (a) and EDS analysis (b) of ZnS thin films annealed at 200°C. Reprinted with permission from Elsevier from Ref. 54.

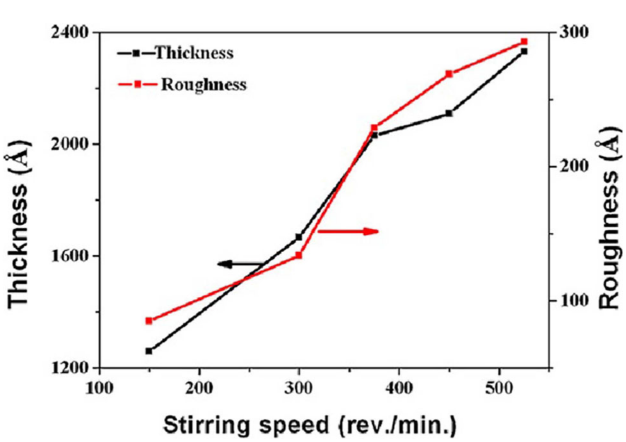

Fig. 5. Thickness and roughness of ZnS films versus stirring speeds. Reprinted with permission from Elsevier from Ref. 60.

unwanted absorption of light is prevented by maintaining the thickness of the window layer with an average growth rate of 100 nm/h. Nature of the material deposited by CBD is solid for which two different types of reactions are possible. One is homogeneous, in which a solid phase is formed within the bulk of the solution, which generally is associated with longer deposition time (> 30 min). The second type of reaction is heterogeneous in which a solid phase is formed at the surface of the substrate. For depositions occurring in short duration (< 30 min), a heterogeneous process exists.

The deposition processes are classified in three different ways: ion by ion, cluster by cluster and mixed mechanism (Fig. 3).[50] In the ion-by-ion mechanism, the deposition process follows a heterogeneous reaction to deposit the film on the substrate and the ions condense on the substrate surface. In

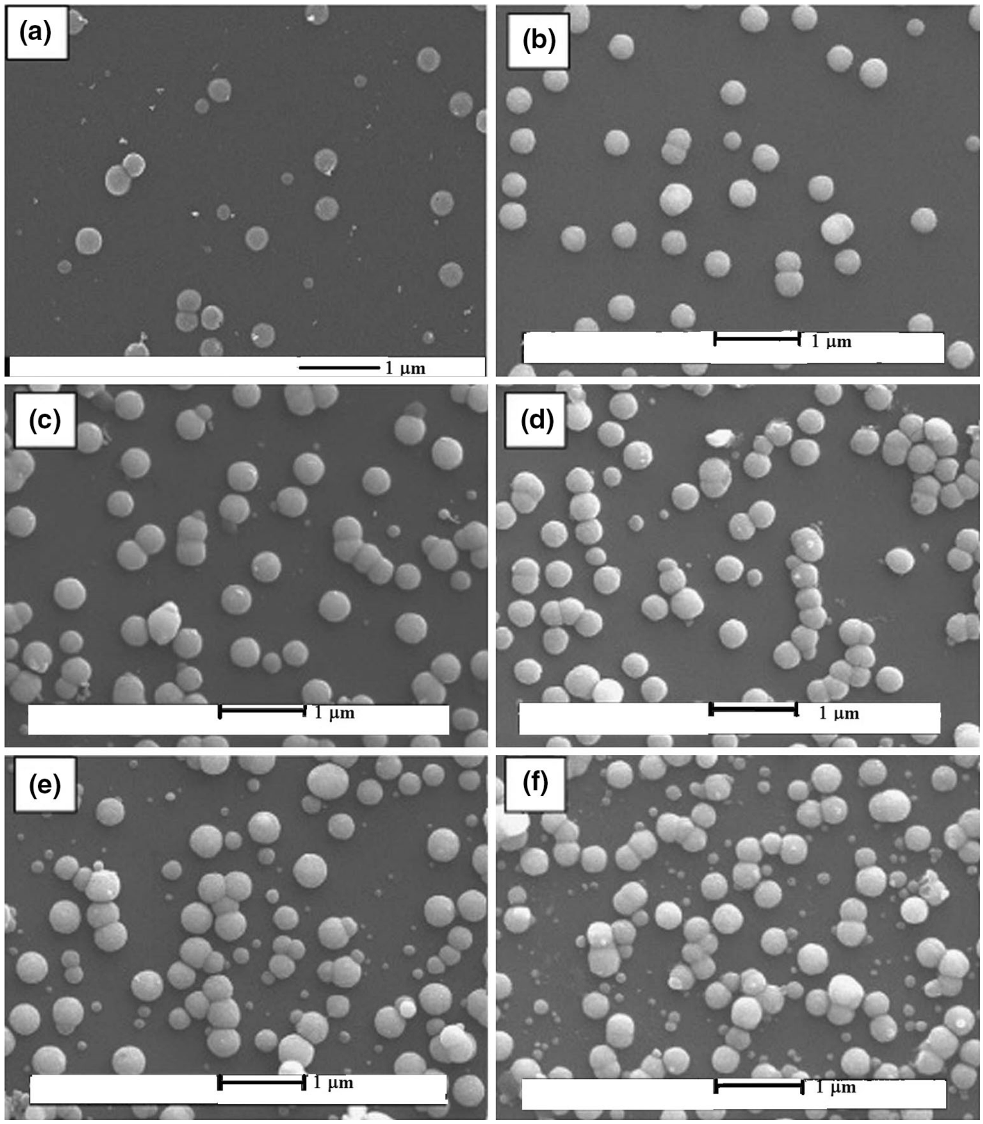

Fig. 6. SEM images of ZnS film prepared with (a) 40 min at a stirring speed of 300 rpm, and (b)–(f) 60 min at a stirring speed of (b) 150 rpm, (c) 300 rpm, (d) 375 rpm, (e) 450 rpm, and (f) 525 rpm. Reprinted with permission from Elsevier from Ref. 60.

the cluster-by-cluster deposition, the process follows a homogeneous reaction such that the particles, which are already formed in the solution, accumulate and occupy the surface of a substrate to deposit the film. In general, both mechanisms exist simultaneously, but which mechanism will dominate the other depends on the nucleation process (i.e., homogeneously or heterogeneously) governed by the time of preparation of the solution. In this situation, where both mechanisms exist in one experiment, the resultant mechanism is called a mixed mechanism.

In order to obtain better results for CBD-grown materials, as well as experimental work, a few mathematical models have also been developed. Reference 51 suggested an approach to the chemical mechanism through the study of the film microstructure for CBD-grown CdS. They presented results of an exhaustive study of CBD-CdS kinetics and proposed a new chemical mechanism which agreed with the kinetic parameters determined by heterogeneous catalysis concepts.

At the end of the twentieth century, Ref. 52 developed a mathematical model on the basis of experimental growth curves of thin films of different materials deposited by CBD technique, and classified different stages in CBD as follows:

i. During the nucleation period, an initial monolayer of the metal chalcogenide is formed on the substrate.
ii. During the growth phase, this monolayer acts as a catalytic surface for the condensation of the metal ions and chalcogenide ions.
iii. When film growth reaches a terminal phase, the film ceases to grow.

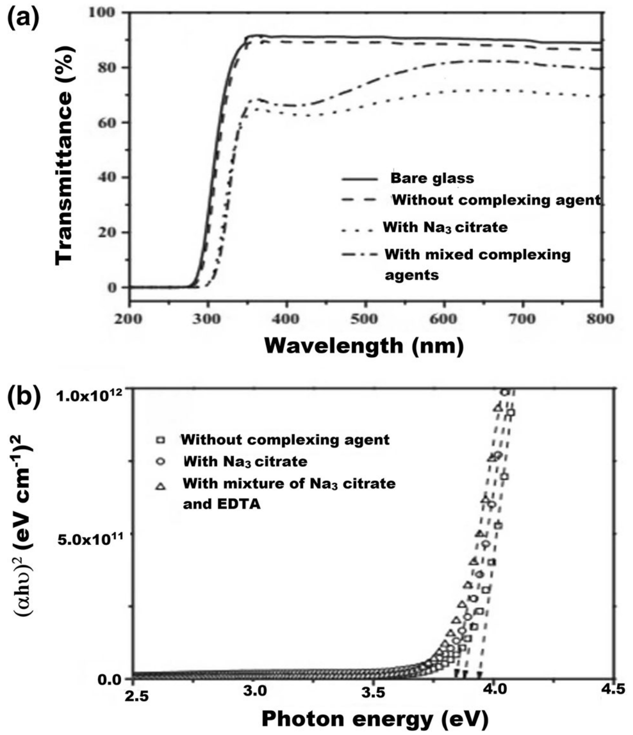

Fig. 7. UV–visible transmittance spectra in the wavelength region from 300 nm to 800 nm (a) and the plot of $(\alpha h\upsilon)^2$ versus photon energy (b) of the ZnS thin films deposited without complexing agents, those with Na_3-citrate and those with a mixture of Na_3-citrate and EDTA. Reprinted with permission from Elsevier from Ref. 62.

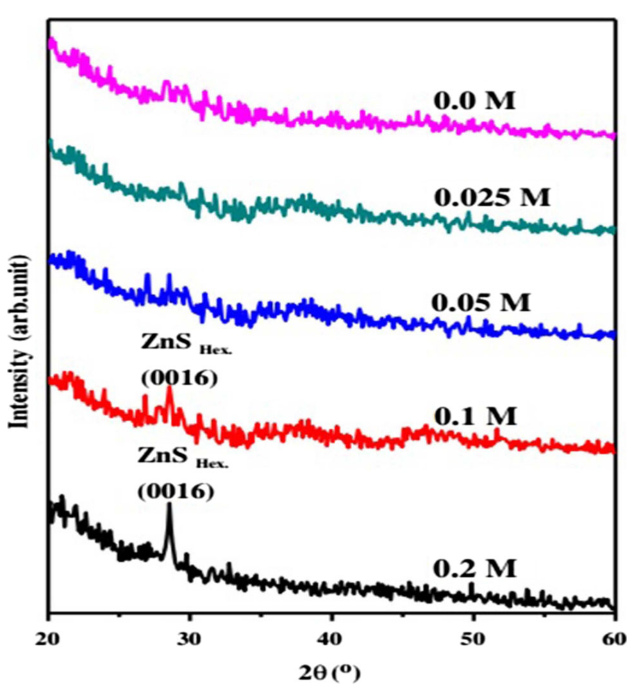

Fig. 8. XRD patterns of the ZnS thin films at different concentrations of Na_3-citrate. Reprinted with permission from Elsevier from Ref. 63.

iv. Duration of induction decreases with increase in bath temperature and bath concentration.
v. An optimum temperature–concentration combination needs to be obtained for maximum film thickness in a given duration of deposition.

Reference 53 developed another computational model for CBD to clarify the effect of the sequence of events during the deposition process on the film growth. Their model was consistent with available experimental data, proving its utility in optimizing various parameters related to the CBD process. There have been a few reports[52,53] on theoretical work undertaken mainly on CdS. The above mechanisms/models are also expected to be equally applicable to ZnS because it belongs to the same group and exhibits similar properties.

PARAMETERS AFFECTING THE PROPERTIES OF ZnS THIN FILMS DEPOSITED BY CBD TECHNIQUE

ZnS has been successfully prepared with crystallite sizes ranging from bulk to nanoscale level, and the structural properties of ZnS were found to be easily influenced by any type of chemical modification. There are various parameters associated with the deposition of ZnS thin films by the CBD technique which strongly affect the structural and optical properties of ZnS. They are discussed in the following sections.

Deposition Temperature

The deposition temperature plays a characteristic role while depositing thin layers with high quality and desired features. There is a close relationship between temperature and thickness of the deposited film. Generally, at lower bath temperatures, the film thickness increases followed by a decrease at higher temperatures. In Ref. 54 ZnS thin films were deposited on a glass substrate by the CBD method and studied for the effects of various parameters. The main purpose of the work was to find the possible influence of temperature on the deposition of ZnS film. For this, they prepared samples at different deposition temperatures ranging from 75 to 95°C for 2 h and annealed them at 200°C. Annealing is a critical treatment in the method of producing uniform films. More about annealing will be discussed in "Effect of Annealing" section. Table II shows the variation in film thickness with increasing deposition temperature. As can be seen, the films show an uneven variation in the thickness when the deposition temperature increases. The same pattern was observed when films are annealed at 200°C. Actually, at lower temperatures, the rate of growth is slow, which quickens at higher temperatures resulting in a greater thickness of the films. However, at still

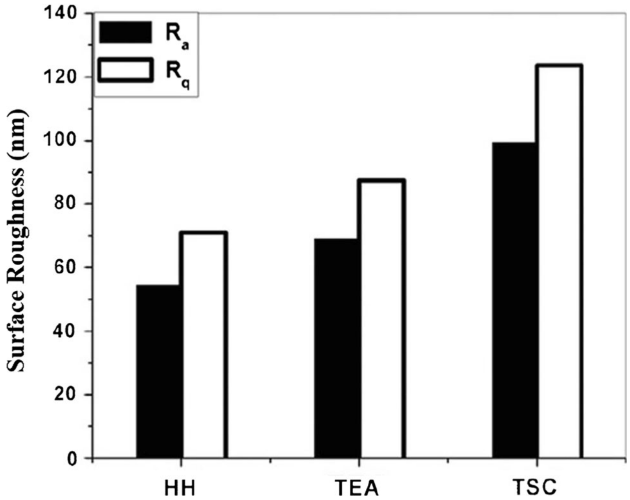

Fig. 9. The average (R_a) and rms value (R_q) of surface roughness of ZnS films. Reprinted with permission from Elsevier from Ref. 64.

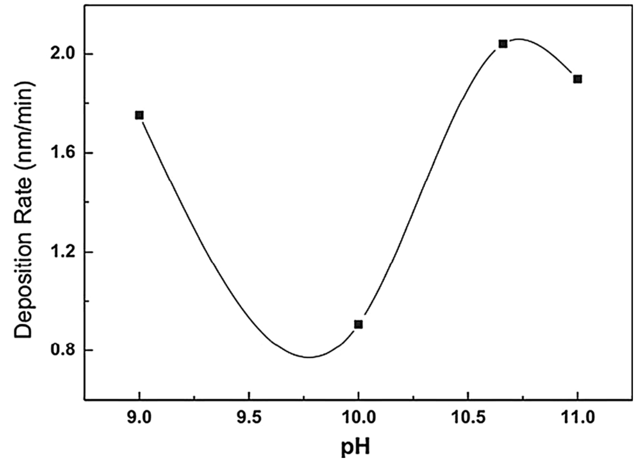

Fig. 10. Variation of ZnS thin films deposition rate as a function of pH solution. Reprinted with permission from Elsevier from Ref. 68.

higher temperatures, when the repulsive force between the grains becomes dominant, film thickness decreases. The authors recorded and analyzed the corresponding transmittance spectra of annealed ZnS films with a spectrophotometer (U-3310) which is an instrument used for the measurement of the amount of light reflected from a material or the amount of light absorbed by it. For the incident light of wavelengths ranging from 350 nm to 800 nm, the researchers obtained more than 75% transmittance for light with a wavelength above 600 nm. The films deposited at lower temperatures contained particles with larger spaces not covered with dense particles. As a result, the transparency of films deposited at lower temperatures was more than that at higher ones. These researchers observed that the thicknesses of films increased when deposition temperature was higher, so that the transmittance fell when the deposition temperature rose.

The results of surface morphology of a sample verify other properties, i.e., optical and electrical. Scanning electron microscopy (SEM), transmission electron microscopy (TEM), and field emission electron microscopy (FESEM) are such techniques, which are of prime importance in this regard. Reference 54 studied the surface morphology of as-deposited ZnS films through SEM (JSM-6360LV). SEM provides images of a material by scanning its surface with a focused electron beam. The atoms of the object interact with these electrons and various signals are produced that contain information about the surface of an object and its composition. In that study, Zhou and co-workers found an increment in the size of particles, and the material showed a dense and ordered morphology corresponding to a higher value of deposition temperature. Thus, it was concluded that, if thin films are deposited at a constant time, an increase in temperature introduces more homogeneity into the process. An analysis of SEM images of unannealed and annealed (200°C) samples showed that the annealed films were more homogeneous and extremely dense. Also, as expected, the distribution of granules was more uniform in the annealed films. Thus, it was concluded that the film surface became smoother and more uniform with some growth in the population of small particles on the surface due to the oxidization of ZnS into ZnO as the annealing treatment was carried out in the air. It was quite possible that the larger particles on the surface were ZnO grains. The unannealed and annealed samples were also compared on the basis of their x-ray diffraction (XRD) patterns. XRD is a well-known characterization technique which is used to determine the crystal structure of a material and, in the case of thin films, it also helps to determine the epitaxial relationships between the film and the substrate. In the present case, the amorphous nature of films was seen. There might be two reasons behind the obtained amorphous nature; either the film deposited on the substrate was very thin or the grains were very tiny and disorganized. Here, it is important to mention that, if the film is very thin ($\sim$ 110 nm) consisting of very few grains, it is difficult to observe any peak in the XRD pattern.

TEM is another electron microscopy technique in which an electron beam is transmitted through a sample to form an image of better resolution than other light microscopes. When TEM images and electron diffraction patterns of annealed ZnS thin films were studied, the authors were surprised to see that the examined ZnS film was sufficiently thin, as it had both Zn and S elements (Fig. 4). This contradiction between the XRD and TEM results was removed by the argument that there were some microcrystallines existing in the samples due to which the diffraction peaks were not present in XRD analysis and amorphous nature was obtained.

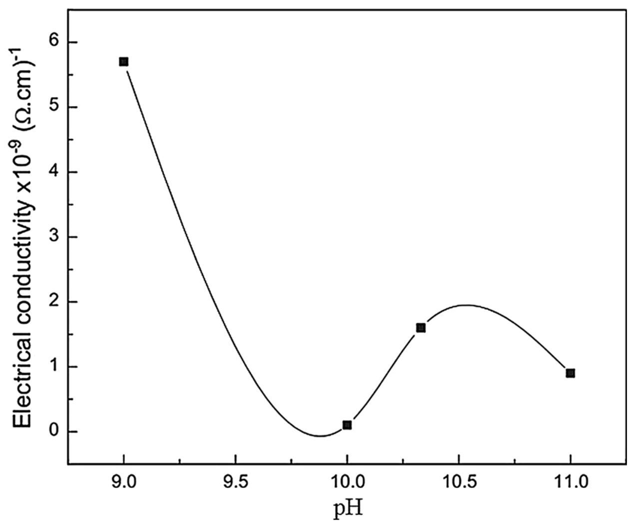

Fig. 11. Influence of pH solution on the electrical conductivity of ZnS thin films. Reprinted with permission from Elsevier from Ref. 68.

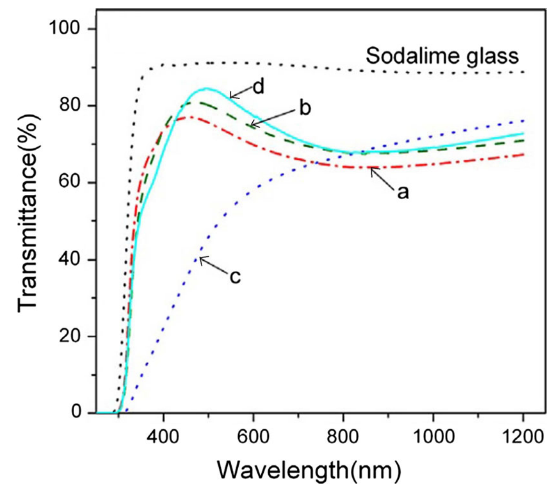

Fig. 12. The UV–visible transmittance spectra of the ZnS films. *a*, *b*, *c* Deposited by the open system at RH = 60%, RH = 70% and RH = 80%, respectively, *d* deposited by the hermetic system. Reprinted with permission from Elsevier from Ref. 71.

Reference 55 also studied the effect of deposition temperature on the properties of ZnS thin films deposited by the CBD technique. The film deposition was carried out at comparatively lower temperatures varying from 50°C to 90°C. These researchers observed that the thickness of the film deposited at highest bath temperature (90°C) was higher than that of the films deposited at the lower deposition temperatures. Surprisingly, they found that the optical transmittance of the thicker film (90°C) was much better, and it was more than 90% in the visible region. Here, it is worth mentioning that the variation in transmittance in different regions (visible or near infrared) mainly comes due to the plasma resonance of electron gas in the conduction band.[56] Another interesting result they witnessed was that the pH value decreased significantly with the increase in deposition temperature. As we know that, with the increase in temperature, the ability of water to ionize in this way increases and thus the concentration of H^+ in solution increases and hence the pH drops.

At the same time, the band-gap energy (E_g) of ZnS thin films varied with the deposition temperature. Initially, it decreased from 4.06 eV to 3.93 eV with the increase in temperature from 50°C to 70°C and, with a further increase in temperature beyond 70°C; it increased from 3.93 eV to 4.03 eV. Still, it was more than the corresponding bulk band-gap value (E_g = 3.7 eV). As explained earlier, the low temperature assists grain growth leading to a reduction in E_g, but when the temperature is still high ($\sim$ 90°C), it hinders single grain growth and the band-gap increases. However, the increase in E_g can also be correlated with the well-known quantum confinement effect. Whenever there is a reduction in particle size ($\leq$ 10 nm), the band-gap is observed to widen. In the present case, the variation in particle size corresponding to different deposition times also led to variation in band-gap values. A few other researchers have also reported that, by increasing the bath temperature, the CBD-ZnS films became thicker, homogeneous and free from pinholes.[57]

Effect of Stirring Speed

In a typical CBD process, in order to ensure a homogeneous distribution of the chemical compounds, a solution is stirred before placing it in a water bath for deposition. This not only reduces the creation of colloidal particles and decreases the grain size of the particles, but absorbs those lying on the substrate, which perturbs the diffusion of particles to the surface. This can be done manually or using a stirrer. According to Ref. 58, stirring speed did not affect the growth rate of ZnS thin films. Reference 59 experimentally verified it and clarified that this was true to some extent. In the beginning, the stirring speed does not have a significant impact on growth rate of ZnS, but for longer deposition times, typically beyond 30 min, the growth rate was directly affected by the stirring speed. Here, we want to comment that stirring may offer some obstacles to producing homogeneous ZnS films: (1) it can reduce the transparency resulting in ZnS films of poor quality; (2) it can hamper the diffusion of complex ions towards the substrate and the adsorption of complex ions on the substrate, and (3) stirring can slow down grain and film growth. As a conclusion, it can be said that necessary care must be taken in stirring the solution to obtain the desired output.

Reference 60 extended the work by Ref. 59 and studied the structural and optical properties of ZnS films deposited on a soda lime glass substrate corresponding to different stirring speeds for longer deposition times (> 30 min). In the case of an unstirred solution, upon rinsing the substrate with

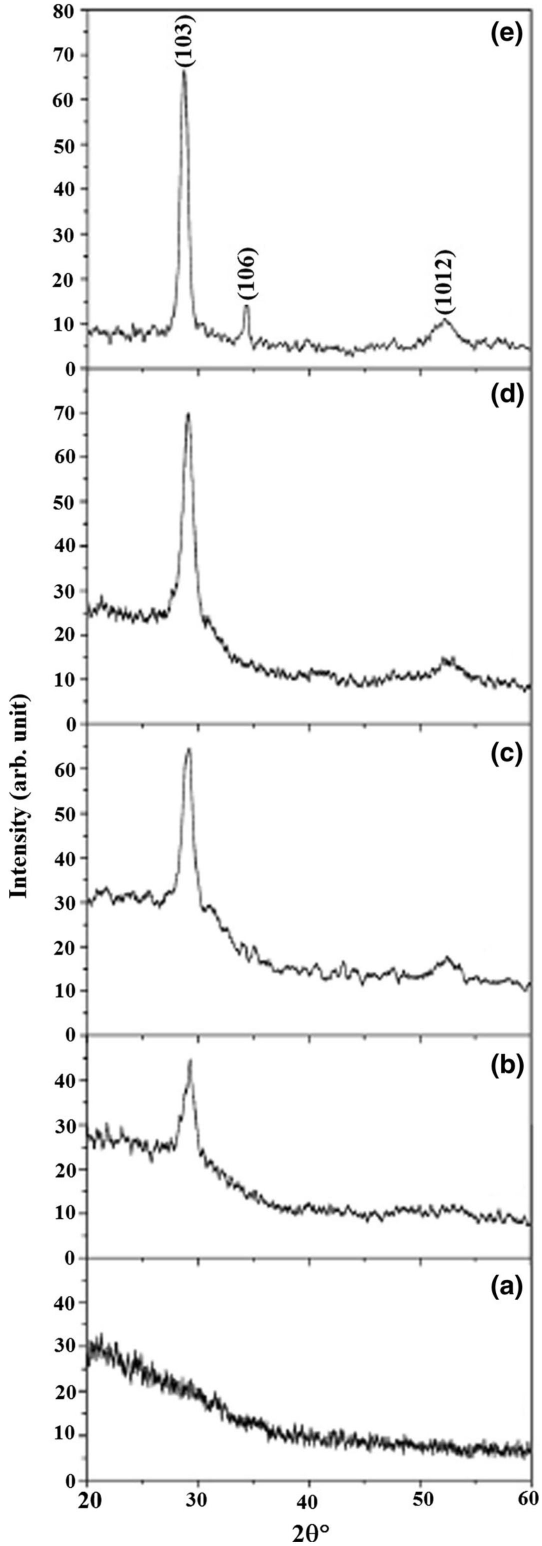

Fig. 13. X-ray diffractograms of thin films (a) as-deposited and when annealed at (b) 200°C, (c) 300°C, (d) 400°C, and (e) 500°C. Reprinted with permission from Elsevier from Ref. 72.

distilled water, the particles were washed out from the surface, which was the reverse of their previous findings. Upon stirring the solution, the increase in

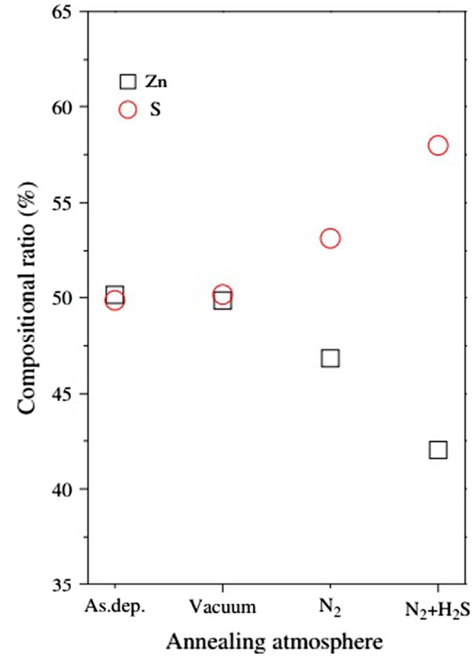

Fig. 14. Elemental analysis of the ZnS thin films annealed in different atmospheres at 500°C for 1 h. Reprinted with permission from Elsevier from Ref. 76.

film thickness was almost linear with increasing stirring speed (Fig. 5). Beyond the linear growth region, the increment in stirring speed helped to improve the growth rate. This could be explained by the fact that, for the unstirred solution, the particles covered the surface randomly while stirring introduced more homogeneity into the deposition process.

The SEM images of as-deposited ZnS films at different stirring speeds and corresponding times are shown in Fig. 6, which clearly indicate the presence of more colloidal particles on the surface with increasing stirring speeds. Reference 60 expected the film to be smoother at higher stirring speeds as it involved growth in the homogeneous process, but the result was different. Many clusters were seen in the SEM images, and the roughness increased linearly with increasing stirring speed. The reason behind this contradiction was associated with different controlling steps in different regions. In the linear region, the chemical reaction governed the growth during the heterogeneous process, while, in the saturation region, physical steps predominated during the homogeneous process.

Another study was carried out to observe thickness variation with two constant stirring speeds, 300 rpm and 525 rpm. For a deposition time of less than 30 min (i.e., a heterogeneous process), the film thickness was almost the same, but when the deposition time was more than 30 min (i.e., a homogeneous process), the thickness was greater. This validated previously obtained results that stirring speed significantly affected the homogeneous process and a higher stirring speed could

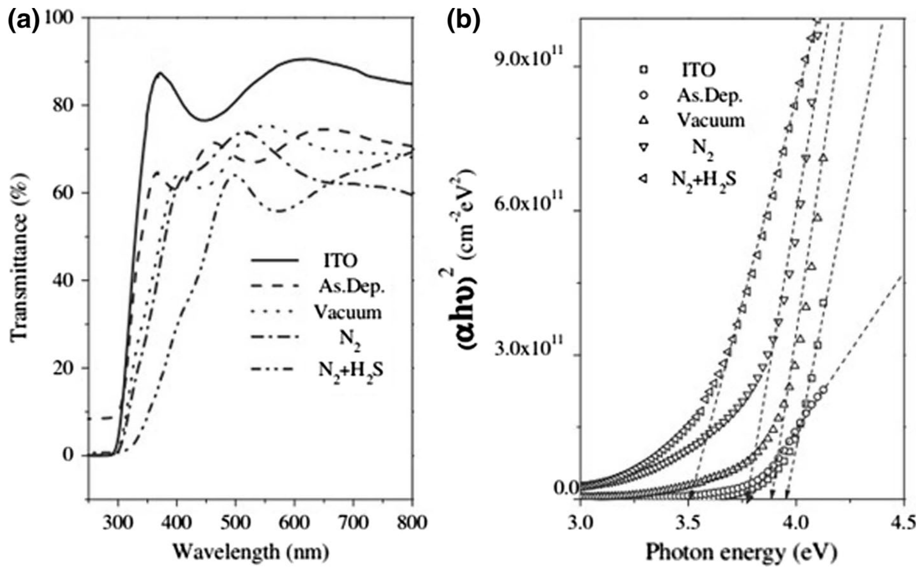

Fig. 15. Visible transmittance spectra in the wavelength region from 300 to 800 nm of the as-deposited and annealed ZnS thin films in different atmospheres (a) and plots of $(\alpha h\upsilon)^2$ versus photon energy of the as-deposited and annealed ZnS thin films in different atmospheres (b). Reprinted with permission from Elsevier from Ref. 76.

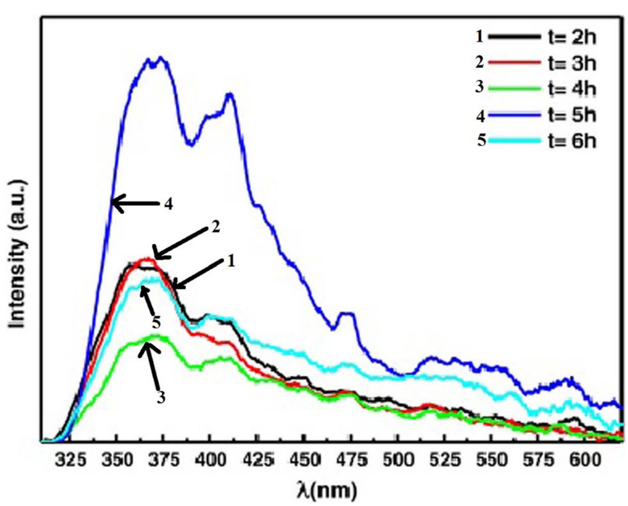

Fig. 16. Band-gap energy versus deposition time of ZnS thin films deposited on glass substrates. Reprinted with permission from Elsevier from Ref. 81.

provide a thicker film. The films showed 70–80% transmittance in the visible region, and the obtained band-gap value was E_g = 3.63 eV. It was also found that the stirring speed did not improve any other structural or optical property of the film. A similar result was obtained by other researchers for CBD-ZnS films prepared with different types of solutions.[61]

Effect of Complexing Agents

One of the major factors which govern the reaction mechanism and improvement in the growth rate for the deposition of ZnS films by CBD is the addition of a suitable complexing agent during deposition. While depositing a film, the complexing agent plays an important role in controlling the concentration of the Zn^{2+} ions. For a long time, ammonia and HH remained the favored complexing agents, but their toxic nature was a major challenge when working with them. Thus, the search for a suitable non-toxic complexing agent started and several complexing agents such as tri-sodium citrate (TSC), tartaric acid, and ethylenediaminetetraacetic acid (EDTA) were used. In this regard, the work carried out by Ref. 62 is noteworthy. They used complexing agents Na_3-citrate and a mixture of Na_3-citrate and ethylenediamine tetra-acetate (EDTA) and studied their effects on the structural, chemical, morphological, optical, and electrical properties of ZnS thin films. In fact, they prepared two solutions in the presence of TSC and TSC-EDTA as complexing agents along with ammonium hydroxide as a pH adjustor. The deposited ZnS films were found to be smoother and more uniform upon the introduction of a complexing agent. In their XRD study, the film deposited without any complexing agent was amorphous in nature while the film with one or more complexing agents showed a crystalline structure with a (111) peak. This result supported the necessity of a complexing agent to improve the crystalline behavior of CBD-ZnS films. In the corresponding transmittance spectra, the films deposited in the presence of complexing agents showed less transmittance as compared to the film deposited in the absence of a complexing agent. This occurred because the film deposited with a complexing agent was thicker in comparison to the film without a complexing agent. Figure 7a and b presents the UV visible transmittance spectra and corresponding Tauc's plots obtained for ZnS films in the wavelength range 200–800 nm. In our view,

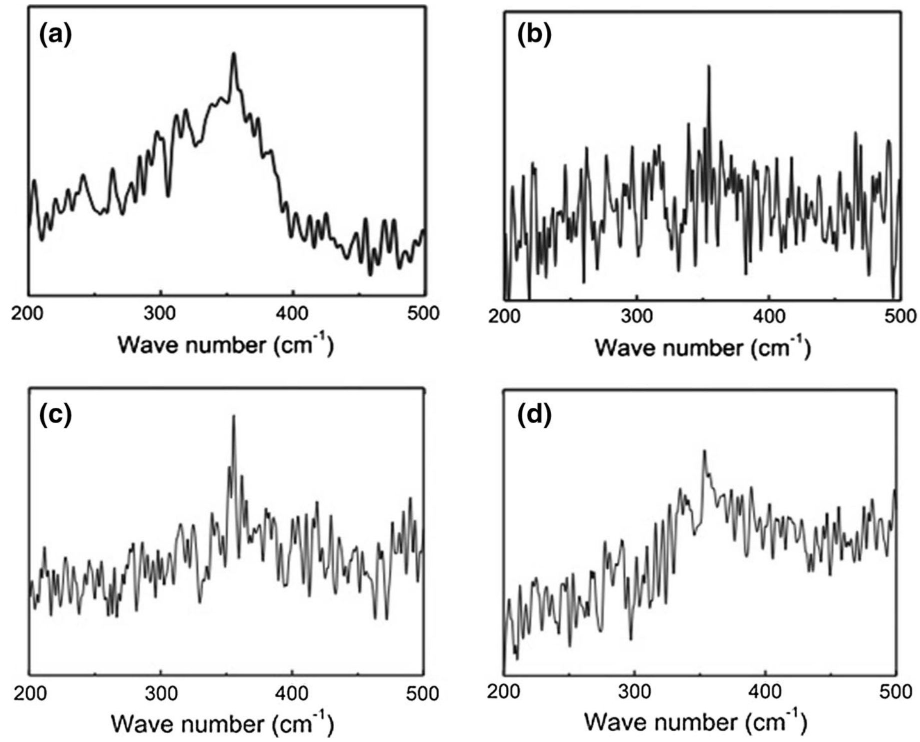

Fig. 17. Raman spectra of annealed ZnS thin films from different zinc salts. a–d correspond to the ZnS-C_1, ZnS-S_3, ZnS-Cl_2, and ZnS-N_2 thin films, respectively. Reprinted with permission from Elsevier from Ref. 77.

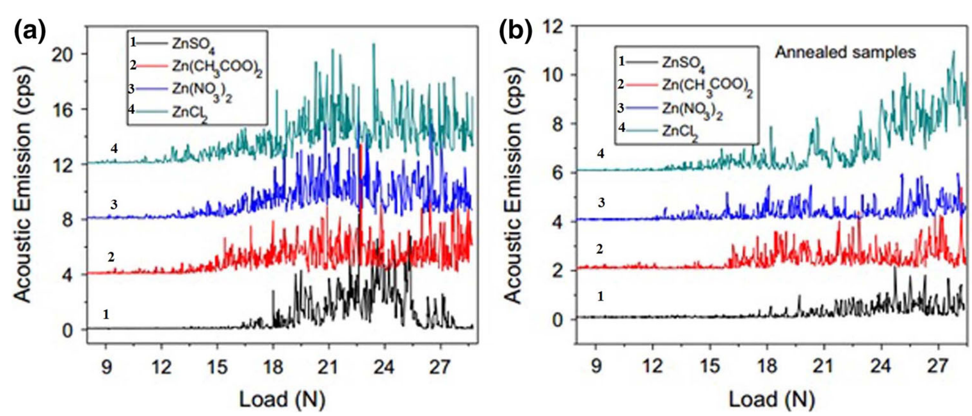

Fig. 18. Scratch testing curves for measuring interface bonding force of as-grown (a) and annealed ZnS films (b) deposited for 2.5 h."Reprinted with permission from Elsevier from Ref. 84.

before recording absorption/transmission spectra, it is pertinent to ensure that the examined film is uniform and smooth throughout. Otherwise, while recording absorption/transmission spectra, the spectrometer will give results corresponding only to the exposed area which may differ from other regions. To obtain a Tauc's plot, a graph is plotted between the incident photon energy and $(\alpha h\upsilon)^2$, and the linear portion of the curve is extrapolated. A point on X-axis is observed by increasing the straight line towards the axis and this point gives the band-gap value. The transmittance values were almost 85%, 65% and 70%, corresponding to films deposited without a complexing agent, in the presence of TSC and TSC-EDTA as a complexing agent, respectively. The morphological behavior of the film after using a complexing agent was uniform and closely packed with the grain size falling in the range 30–100 nm.

In their study, Ref. 63 used TSC (0 M to 0.2 M) as a sole complexing agent and investigated the possible effects on various properties of CBD-ZnS. FESEM investigations showed that the concentration of TSC influenced the morphological behavior,

Table III. Some important parameters and their effects on various properties of CBD-ZnS films

Parameters	Affected properties
Deposition temperature	Thickness, optical transmittance, band-gap, pH of solution, morphology
Stirring speed	Thickness and roughness, film growth rate
Complexing agent	Crystalline behavior, optical transmittance, thickness and roughness, morphology
pH value	Crystalline behavior, optical transmittance, band-gap, film growth rate,
Humidity	Crystalline behavior, morphology, optical transmittance
Annealing	Morphology, crystalline behavior, optical transmittance
Deposition time	Crystalline behavior, thickness, band-gap
Zinc salt and [Zn]/[S] ratio	Morphology, crystalline behavior, film growth

and controlled the thickness of the deposited film. An increase in the concentration of TSC resulted in the reduction of the film thickness. XRD patterns indicated that, for a lower concentration of TSC, the film presented an amorphous structure, whereas it exhibited crystalline behavior when the TSC concentration was increased from 0.1 M to 0.2 M (Fig. 8). From this result, we infer that, to deposit a film with a good crystalline structure, there is a lower limit to the addition of a complexing agent. Apart from the above, the optical transmittance in the visible region was between 75% and 85% with 0 M and 0.2 M TSC, respectively, due to the reduction in the thickness of the film. We suggest that a ZnS film with 85% transparency in the visible region can be employed for fabricating an AC thin film electroluminescence (ACTFEL) device.

Reference 64 used different complexing agents such as HH, ammonia, and TSC along with TEA to obtain homogeneous ZnS thin films. One of the major problems associated with CBD-ZnS thin film was the possible existence of hydroxide and oxide of zinc, and ligands like HH, TEA, and TSC suppress their formation by means of giving a more stable complex with zinc. In the CBD process, complexing agents bind those metal ions, which are necessarily required to minimize the homogeneous precipitation of the compound. The reaction mechanism either involves ion by ion deposition or cluster by cluster deposition. Reference 64 suggested a mechanism in which the cluster by cluster mechanism was accompanied by the ion by ion mechanism when TSC was used as a complexing agent, and this mixed mechanism was found to be responsible for greater thickness and more roughness on the surface of a film. In the surface morphology of ZnS thin films studied by atomic force microscopy, surface roughness was found to increase, while the grain size calculated by Scherrer's formula showed a decrese when complexing agents were used in the sequence HH, TEA, and TSC. The comparative chart plotted for surface roughness is shown in Fig. 9. As noticed from the chart, the surface roughness was lowest for ZnS film prepared using HH as a complexing agent. During the deposition, the released zinc ions travel with such a moderate speed that the adsorbed ions become diffused and became homogenized before the beginning of nucleation of the second layer. This was the reason due to which the surface layer became smoother for films deposited with HH as a complexing agent. Similarly, zinc ions were observed to be released too quickly in the presence of TSC as a complexing agent, and consequently the surface roughness was more than that of HH. The grain sizes for films in the presence of HH, TEA, and TSC were estimated to be 66.7 nm, 34.4 nm, and 24.9 nm, respectively. The decrease in grain size for TSC-added films can be explained by the fact that the adsorbed molecules could not diffuse to the surface because they had not had enough time due to the higher release rate of zinc ions. The film deposited using the solution of HH and ammonia as a complexing agent was more uniform and smoother, being thinner in comparison to the film deposited with the other two complexing agents. The observed band-gap value was 3.37 eV with 87% transmittance in the visible region. These properties of CBD-ZnS film are helpful for it to be a suitable buffer layer for CIGS thin film solar cells. However, the other two films deposited in the presence of TEA-TSC and TSC-ammonia showed medium and low transmittance due to their greater thickness, but they exhibited excellent luminescent properties. Reference 65 also performed an experiment to study different properties of ZnS films with varying concentrations of HH, and found dense, homogeneous and adherent films with increasing full width at half maximum (FWHM) and band-gap value when the concentration of HH was increased from 0 M to 2.5 M.

Effect of pH Variation

pH is another major factor that affects the properties of CBD-grown ZnS. One of the advantages of CBD is that the nucleation and growth of particles can be controlled during the synthesis process through this method. The pH of the solution appears to be a critical parameter for the phase formation, particle size, and morphology of the structure during the solution method. The size and size distribution of nanoparticles can be controlled by varying the pH value. A literature survey[62–64,66,68] indicates that the effect of pH on the morphology and properties of ZnS films is rarely an important factor in determining the quality.

Reference 66 investigated the possible effect of pH variation on various properties of ZnS deposited by CBD. In the presence of ammonia as a pH adjuster, the pH value was varied between 10 and 11.5. For a pH value of 10, the XRD pattern exhibited two peaks, at 28.80° and 47.7°. When the pH value increased further ($10 < pH < 11.5$), a compromised crystalline behavior was found, and finally, for 11.5 pH, the characteristic peaks disappeared. This proved that the pH 11.5 value of the solution disturbed the crystallinity of the material. A close observation of the optical properties revealed that the transmission increased with the increase in pH for the wavelength range 300–1800 nm. The film deposited with the lowest pH (10) was the most crystalline, but it had the least transmission value of almost 20–46% in the visible region, whereas the film deposited at pH 11.5 showed the best transmittance, which was between 55% and 70%, but the nature of this film was poorest among them all. Lower pH values were associated with higher growth rates, so, with lower pH values, the number of OH^- ions formed in the solution was increased, resulting in the production of more $Zn(OH)_2$. Due to this fact, the Zn ions became insufficient for desirable ZnS growth. So, the films with pH 10 were thicker than the films having pH 11. When the pH value increased from 10 to 11.5, the band-gap value decreased from 3.78 eV to 3.67 eV. A similar result was obtained by Ref. 67.

Reference 68 further studied the effect of pH on the deposition rate and electrical conductivity of ZnS thin films. In their study, during the deposition of ZnS thin films by CBD, HH was used to maintain the pH between 9 and 11. For different pH values, the growth rate was observed to vary between 0.9 nm/s and 2 nm/s, showing minima at pH 10. At this pH value, the rate of deposition was low due to the higher solubility of ZnS. HH helped to maintain the solubility of ZnS with a slower rate that provided better growth condition. When the pH value increased further (pH 10), the deposition rate increased due to the presence of more oxides that were introduced to achieve better formation of ZnS (Fig. 10). ZnS films prepared by the CBD technique using popular complexing agents such as ammonia and HH are either amorphous or poorly crystallized. Therefore, annealing is generally preferred to improve the film crystallinity. Also, in the present case, the as-deposited films were almost amorphous in nature and, upon annealing at 550°C, they showed a better crystalline structure. These researchers faced the common problem of the coexistence of ZnO and Zn $(OH)_2$ as they found another peak in the XRD pattern of the annealed films with pH 11. This was in good agreement with another reported result.[97] Reference 68 found electrical conductivity to be significantly affected by the pH value. Due to changes in the pH value of the solution, the growth of the films was disordered and the electrical conductivity was altered (Fig. 11). When disorder in film growth increased, a large number of defects were introduced due to which the concentration and mobility of the free charge carriers were reduced. Thus, the electrical conductivity decreased.

Effect of Humidity

Humidity in the environment also affects the growth, quality, structural, and optical properties of films deposited by the CBD technique. A typical CBD process can be performed in an open system, where the reaction receptacle is open to the environment, or it can be performed in a closed system in which the reaction vessel is contained.[58,69,70] In a hermetic CBD system, the volume of the system is restricted in such a way that the system is in thermal equilibrium, and the interface between the bath and the substrate is interfered with as little as possible. On the other hand, in an open CBD system, the gas–liquid interface is interfered with by environmental humidity. Both systems are depicted in Fig. 2. The exposure of the CBD system to the environment may trap moisture and affect the quality of the deposited film. Even after deposition, the quality of the films, owing to their colloidal nature, is generally substantially degraded. Although humidity control is essential for producing defect-free thin films, no systematic study about the effect of humidity on the growth characteristics and properties of CBD-ZnS thin films were reported until Ref. 71 published results of an exhaustive work on the effects of humidity on the growth characteristics and properties of ZnS films deposited by CBD. Their analysis was based on the comparison of results obtained from both open and hermetic CBD systems. In the experiment, the first reaction container was a 250-ml beaker that was used for the open system while a capped bottle was employed for the hermetic system. The values of relative humidity (RH) in the environment corresponding to the open CBD system were 60%, 70%, and 80%.

Reference 71 found the surface morphology of the films to be very delicate due to the relative humidity in the environment as the films deposited at RH 70% were appreciably compact and continuous, whereas the other two films corresponding to RH 60% and RH 80% were obtained with a powdery surface showing some cracks. The XRD study revealed that, in comparison to poorly crystalline films prepared with the open system, the film deposited via the hermetic system showed an improvement in crystalline behavior. In the case of an open system, when the humidity level in the environment increased, a large number of hydrogen ions were introduced into the bath and carbon dioxide was dissolved so that the number of Zn^{2+} ions increased in the solution, and might be precipitated to form zinc oxide. This was the reason for the existence of a large amount of unwanted ZnO particles. However, the amount of carbon dioxide in the hermetic CBD system was limited and the environment could not interfere to increase it. In this way, the formation of ZnO was limited in the hermetic system leading to better crystalline structure. Figure 12 shows the transmittance spectra of ZnS films in the wavelength range 200–1200 nm deposited by the open system at different values of relative humidity. As reported by Ref. 71, the visible transmittance reduced due to humidity in the environment. For ZnS film deposited by a hermetic system, an average visible transmittance (77%) in the wavelength region 400–800 nm could be derived, which was the best among all the samples. Thus, it was concluded that the film deposited by the hermetic CBD system had better transmittance as compared to the samples deposited by the open CBD system.

Effect of Annealing

All the parameters which we have discussed earlier were monitored before or during the deposition process so that they might be responsible for the improvement or disturbance in the growth of a film. Annealing of CBD-grown thin films is the only factor which affects the quality and the properties of the films post-deposition. It helps to improve the crystallinity, morphology, and optical properties of a pre-deposited film. Different kinds of film require a heat treatment at different temperatures (200–550°C) and at different stages. Upon annealing in air, the films become smooth and uniform due to the removal of disturbing particles from the surface by thermal energy. In order to improve various properties of ZnS thin films, annealing has been preferred by many researchers, the details of which are summarized in Table I.

In the XRD study of ZnS thin films in the temperature range from 200°C to 500°C, Ref. 72 observed that, as the annealing temperature increased from 200°C to 500°C, the crystallinity of the material improved drastically (Fig. 13). Annealing improves the crystallinity of films, and also brings morphological changes. The same was noticed by Ref. 72 when they scanned ZnS thin film annealed at 500°C. The film was uniform, smooth and crack-free as compared to the unannealed film. Many researchers have annealed the ZnS film in their investigations of the influence of different parameters on the various properties.[54,68,73,92–94] Some researchers have worked to remove CdOH or ZnOH phases by annealing treatment and have obtained an improved crystalline behavior.[73] The variation in different properties of ZnS thin films due to annealing in different atmospheric conditions, such as vacuum, H_2, N_2, Ar_2, and H_2S, has also been reported.[74,75]

Apart from heat treatment in air, annealing can also be performed in vacuum and controlled atmospheres such as with endothermic gas (a mixture of carbon monoxide, hydrogen gas, and nitrogen gas). Annealing is also carried out in forming the gas, a mixture of hydrogen and nitrogen. A similar kind of work was reported by Ref. 76 in which they presented the effect of various annealing conditions on the properties of ZnS film deposited on an ITO-coated glass substrate by the CBD method. The annealing was carried out in vacuum, N_2 and, $N_2 + H_2S$ atmosphere for 1 h in the temperature range 300–500°C. In another experiment, films were annealed at 500°C for 30–120 min in a $N_2 + H_2S$ atmosphere. In the XRD pattern, the films annealed in N_2 and vacuum were either non-crystalline or poorly crystalline. On the other hand, the films deposited in the $N_2 + H_2S$ atmosphere were well crystallized at the annealing temperature of 500°C and the major peak (111) showed an increase in intensity when the annealing temperature approached 550°C. It was concluded that the thermal energy might be responsible for the improved crystalline nature. Increases in the intensity of XRD peak can be understood on the basis that, when a sample is heat-treated, the impurities and artifacts escape from the film surface making it defect-free.

Figure 14 shows the variation of composition ratio with annealing atmosphere. In vacuum, the composition of Zn and S was almost equally balanced, but in the N_2 and $N_2 + H_2S$ atmospheres the existence of sulfur exceeded the zinc concentration. The reason behind this variation was attributed to two factors. First, the H_2S gas raised the amount of sulfur, and secondly the Zn atoms were vaporized by thermal energy, resulting in an increment in the quantity of S over Zn. The transmittance spectra of ZnS thin films in the wavelength range 300–800 nm is shown in Fig. 15. As is evident from the figure, the transmittance in the visible region for the films annealed in vacuum and N_2 atmosphere was better than that of the films annealed in $N_2 + H_2S$ atmosphere. It was due to the removal of some small particles, which acted as scattering centers. Reference 77 reported that the annealing treatment of CBD-ZnS films in Ar/H_2S atmosphere helped in the excess of S due to the conversion of ZnO or $Zn(OH)_2$ into zinc sulfide.

Effect of Deposition Time

Among the various parameters affecting the growth rate and properties of ZnS thin films deposited by the CBD technique, deposition time is probably the most important factor. It affects almost every property of ZnS thin films including film growth, thickness, crystalline behavior, surface morphology, and optical.[78,79] In fact, it is all about optimization of deposition time and temperature while producing good-quality and adherent ZnS films through CBD. While analyzing the XRD patterns of PbSe films deposited at different times, Ref. 80 found that, for the deposition times of 30 min and 60 min, the crystallites had a preferred orientation along the (111) plane, whilst for the deposition time of 45 min, the crystallites had a preferred orientation along the (200) plane. This indicated that the orientation of the grain growth along different directions was dependent on deposition time. Another interesting observation was the increase in the number of peaks appearing in the XRD pattern with increasing deposition time, indicating an improvement in crystalline nature. For longer deposition times (> 60 min), the films were non-adherent and were washed out.

Reference 81 synthesized ZnS films by CBD but for longer deposition times (2–6 h) and studied the related effects. In the XRD patterns, the group of researchers observed that the deposition time affected the crystal quality of the film. All diffraction patterns exhibited the hexagonal WZ structure with significantly broad peaks. Films deposited at lower deposition times (2 h and 3 h) were found to be poorly crystallized, and an unwanted ZnO phase existed in the spectra of the film deposited for 2 h; however, for the deposition time of more than 3 h, all these problems were sorted out due to the sulfidation process and subsequent growth of ZnS crystallites. These results were in good agreement with the findings of Ref. 80. However, in the latter case, the intensity of the peaks increased with increasing deposition time even beyond 3 h. This was because, in the beginning, the formation of some ZnO nuclei took place and S^{2-} ions became arranged in their neighborhood. When the deposition time increased further, the ZnS–ZnO interface supported the diffusion of oxygen ions so that the ZnO phase was removed from the XRD pattern and ZnS crystalline phase improved significantly. The particle size increased from 2.6 nm to 10 nm when the deposition time was increased from 4 h to 6 h, because the nucleation of ZnS stopped as the deposition time was increased further, and the growth of the film followed the increment in average particle size. As a concluding remark, it can be said that the deposition of smooth and adherent thin films is time-dependent but only to some extent. Beyond a particular deposition time, which differs from material to material, deposition of a film is not possible.

Reference 73 also studied the effect of increasing deposition time on the surface morphology of ZnS films. As observed by them, for 2 h deposition, the quality of the deposited films was not satisfactory as the films were not smooth, uniform and crack-free. However, for longer deposition times (> 3 h), homogeneous and heterogeneous deposition processes existed simultaneously, with the morphology showing appreciable compactness. For a deposition time close to 6 h, the heterogeneous process dominated the homogeneous process and the film thickness increased linearly, but for 6 h of deposition, the film thickness decreased drastically from 610 nm to 530 nm.

Figure 16 illustrates the photoluminescence (PL) spectra (recorded by a PerkinElmer LSB 50 spectrophotometer at RT) of the CBD-ZnS single layer thin films deposited for different durations. All the PL spectra exhibited peaks at 365 nm, 410 nm, and 470 nm. As can be seen from the figure, the intensity of the UV-blue emission of the ZnS thin film deposited for 5 h was two times more than that of the samples deposited for 2 h, 3 h, and 6 h. However, the green emission of the films deposited for 5 h and 6 h was more pronounced than that of the other samples. Also, the smallest UV-blue emission intensity was recorded for the ZnS thin film prepared for 4 h of deposition time. Such a decrease in UV-blue intensity was caused by the increase in non-radiative emission at the grain boundaries of the sample deposited for 4 h. This result was in agreement with the work reported by Ref. 82. The PL peaks centered at 365 nm might be due to the band-to-band transition in the ZnS crystallites, while the emission at 470 nm was probably due to sulfur vacancies. The blue emission centered at about 440 nm was assigned to zinc vacancies.[83] Thus, it proves that not only are the structural properties of a material influenced by deposition time but the optical properties are also affected.

Effect of Zinc Salt

Up to now, we have seen that, in the past two decades, enormous efforts were made in the choice of optimum concentration, complexing agents, deposition mechanism, change of pH, and improvement of the crystallinity of ZnS films. Only a few groups employed two different zinc salts as the Zn^{2+} ion sources to acquire CBD-ZnS films. The ZnS thin films were prepared using $Zn(NO_3)_2$ and $ZnCl^{2+}$. Choosing a suitable precursor is another very important factor that affects the quality and properties of CBD-ZnS films. As the deposited CBD-ZnS films, in addition to ZnS, also contain $Zn(OH)_2$ and ZnO, it was difficult to detect them as ZnS(O, OH).

Reference 77 studied the effect of four zinc salts [$ZnCl_2$, $ZnSO_4.7H_2O$, $Zn(NO_3)_2.6H_2O$ and $Zn(CH_3COO)_2{\cdot}2H_2O$] on the structural and optical properties of CBD-ZnS films. The authors found that one of the samples delivered increments in thickness for the first two deposition cycles, but when the number of deposition cycles increased further, the rate of increment in thickness decreased due to saturation in film growth and lack of availability of good coverage for longer deposition. Keeping all the conditions the same, as already explained above, the particle size of the films increased with increasing the deposition rate. Although this led to the emergence of larger-sized particles in ZnS films deposited from $Zn(CH_3COO)_2$

at the highest deposition rate, these films did not show any Raman spectra due to the fact that the quality of the deposited films was poor and their thickness was insufficient. In order to improve the texture, the films were annealed at 500°C for 1 h in an Ar/H_2S atmosphere. The authors also studied the Raman spectra of the films (Fig. 17). Raman spectroscopy is a helpful technique to observe the vibrational or rotational mode of a system. In this technique, a monochromatic light source (usually a laser) is made to shine on a material and the scattered light is detected for the identification of a sample. In Fig. 17, the peak identified at 355 cm^{-1} indicated the presence of cubic β-ZnS in the examined films. Further, the smallest FWHM corresponding to the film deposited using $ZnCl_2$ indicated that the quality of this film was superior to the films prepared with other salts. Thus, based on these results, the researchers concluded that $ZnCl_2$ was the best precursor for the deposition of ZnS films.

Reference 84 used four different zinc salts, $ZnSO_4{\cdot}7H_2O$, $Zn(CH_3COO)_2{\cdot}2H_2O$, $Zn(NO_3)_2{\cdot}6H_2O$, and $ZnCl_2$, along with thiourea as S^{2-} ion source and ammonium hydroxide and HH as complexing agents to deposit ZnS films by CBD. A comparison of various properties of films prepared in the presence of different precursors revealed that the morphological properties of ZnS films were much better for films deposited using $ZnSO_4$, which improved further by annealing treatment. It was assumed that the $SO_4{}^{2-}$ anions helped the precursors to be adsorbed and diffused towards the substrate and was the preferred ion-by-ion mechanism for the growth of film followed by the heterogeneous process. On the other hand, the results indicated that CH_3COO^- and $NO_3{}^-$ not only disturbed the adsorption and diffusion but promoted the cluster-by-cluster mechanism as well. Films deposited using $ZnSO_4$ showed better adhesiveness, specular reflectivity, and homogeneity as compared to films deposited from other Zn-ion sources. It may be noted that better specular reflectance is a sign that the film is smooth and well deposited. This film was crack-free, more compact, and had higher numbers of fine grains. Also, the adhesion strength of CBD-ZnS film deposited using $ZnSO_4$ was more than 30% better than that of films deposited with other Zn ion sources. Annealing at 250°C further improved all the morphological properties of ZnS. The values of adhesion strengths calculated for ZnS films deposited with different precursors were 18.0 N, 15.4 N, 15.1 N and 13.3 N, respectively (Fig. 18). It was evident that ZnS film deposited using $ZnSO_4$ was the most adherent with the substrate when the applied load varied between 0 N and 30 N. These findings agreed well with the FESEM images and growth mechanism of ion by ion deposition. Upon annealing in air at 250°C for 4 h, the adhesion strengths of ZnS films deposited from $ZnSO_4$ and $Zn(CH_3COO)_2$ grew to 19.0 N and 16.0 N, respectively. Based on these experimental findings, the researchers concluded that $ZnSO_4$ and $Zn(CH_3COO)_2$ were capable of improving the mechanical properties of ZnS thin films when deposited properly.

On the basis of their observations, Ref. 84 claimed that the film thickness and deposition rate were better for films corresponding to $SO_4{}^{2+}$ ions. In their structural analysis, the CBD-ZnS films showed poor crystallinity, which improved after multiple depositions. In addition, ZnS film deposited from $ZnSO_4$ had better optical transmission with a blue response. This was one of the excellent characteristics of a film to be used in CIGS solar cells. The transmittance of a film is an important characteristic for solar cell applications. Reference 85 continued this work and reported an enhancement in the quality of ZnS films by co-depositing the film from two zinc ion sources.

Apart from all the parameters discussed above, variation in [Zn]/[S] ratio is another factor that needs attention while depositing CBD-ZnS films. Reference 70 performed a set of experiments to study the effect of variation in [Zn]/[S] ratio keeping volume of other elements constant. The authors found that, when the quantity of the zinc ion source was too high or too low as compared to the sulfur ion source, the chances of depositing ZnS films decreased drastically. It was further observed that for [Zn]/[S] ratios 1:9 or 3:1, the substrate was left blank and the formation of the film was not successful. The ZnS films could be deposited only in the range of the [Zn]/[S] ratio from 1:6 to 1:1 and this proved that the film growth depended on the quantity of precursors used. In morphological studies, the researchers found that the grain size faced a decrement by increasing the [Zn]/[S] ratio from 1:6 to 1:1 as a further increment of the Zn-ion source was not favorable for the growth of CBD-ZnS films. Better optical transmission in the visible range was recorded by minimizing the [Zn]/[S] ratio. In order to provide a brief description, all the parameters and their possible effects on different properties of CBD-ZnS films are presented in Table III.

APPLICATIONS AND FUTURE ASPECTS

The ZnS films offer plenty of applications in the field of materials science due to its fantastic electrical and optical properties. Many researchers have successfully applied these films in various fields for the last two decades. Some notable applications of ZnS thin films are:

i. ZnS films are one of the best suitable semiconducting film materials to be used as a buffer layer in CIGS solar cells.[86]
ii. ZnS films have been successfully applied as an antireflection coating in different types of solar cells.[87]
iii. ZnS films doped with different activators have proved their potential applicability in EL devices.[88]

iv. ZnS films have helped to improve the quality of light-emitting diodes (LED) when used as an active layer.[89]

Apart from the above applications, ZnS films are extensively employed in photodetectors, photoconductors and different types of sensors.[90,91] In the last few years, homogeneous ZnS thin films have been prepared by the CBD technique with improved structural and optical properties. The use of higher-quality CBD-ZnS films is likely to increase in the field of solar cells, optoelectronic devices and diode lasers in the near future. Hence, it is imperative to investigate the effects of some other non-toxic complexing agents on the preparation conditions of CBD. The effect of the above agents can also be examined on photovoltaic cell performance, photoresistance, and photoconductivity. A similar study could be performed by varying the pH value in different ranges different from reported those here. Experiments should also be carried out to fabricate low- cost and more efficient solar cells. A comparison of results can be carried out between various properties of films deposited by CBD and other costly physical techniques. Improvement in the optical properties of ZnS films can lead to their application in CIGS solar cells.

However, there are some limitations associated with CBD techniques. A researcher must be careful while choosing a substrate that does not react with the reaction mixture. So, one should go with updated versions of soda lime or ITO/FTO-coated glass for deposition. If a researcher is going to perform multilayer depositions by the CBD technique, then the problem of undesired reactions between previously deposited layers with the solution prepared for the deposition of a new layer may occur. In order to resolve this problem, the researchers must select the order of deposition of the layers. Also, repeated dipping can enhance the thickness of the film only up to few microns. So, if a researcher needs thicker films then he/she must consider the parameters such as stirring speed, deposition time, and bath temperature, which can help to improve the thickness of the film. Another problem associated with CBD is that the solution is discarded after every deposition. The precipitate can be filtered out and made to react with acids or other suitable reagents so that the starting material can be retrieved and used for further deposition. Thus, these matters need to be given due attention when depositing ZnS or any other semiconductor films by the CBD technique.

Current demand for green and renewable energy has compelled scientists to undertake new challenges worldwide. Because of this, great consideration in future is expected towards thin film photovoltaics. With the advancement of technology, eco-friendly and economically cheaper materials are needed in future. In addition, less costly and more energy efficient techniques also need to be developed. In this scenario, CBD-ZnS films are likely to receive more attention. Pure and transition metal-doped ZnS can be helpful in applications such as LEDs, gas sensors, and laser screens.

SUMMARY

In this review, we have attempted to give an account of recent investigations on CBD-ZnS thin films along with the influence of various parameters affecting their quality and properties. The ZnS films deposited by CBD have become one of the most suitable materials for industrial and research purposes. CBD is a very good technique for the deposition of semiconductor films on an appreciable large area of the substrate. Three different deposition mechanisms, namely ion by ion, cluster by cluster, and a mixed mechanism, are reported to be involved in the CBD technique and, in general, the mechanism existing at the time of deposition and the nucleation process decides the superiority of one mechanism over another. The variation in deposition temperature at constant deposition time results in the variation in thickness of the film and the transmittance, surface morphology, crystallinity, and energy band-gap of the material. Upon increasing the speed of stirring, one can get an improvement in the film growth to obtain a thicker film only for the homogeneous process, but for a lower deposition time ($<$ 30 min), stirring speed did not lead to a significant variation in film growth. In order to prepare ZnS thin films, the use of a complexing agent is mandatory to obtain a uniform, smoother and well-crystalline film. The increment in pH value of the solution is responsible for the disturbance in the crystalline behavior of the film. The growth rate of films was better at low pH values. The band-gap value shows a decrement upon increasing the pH value. Humidity affects the film quality and optical properties of ZnS thin films in the open CBD system. Annealing of ZnS films is found to improve their crystalline nature, surface morphology, and optical properties. When the time of deposition increases, the problem of the existence of the unwanted ZnO phase is overcome. The thickness and growth rate are controlled by increments in the deposition temperature. $ZnCl_2$ and $ZnSO_4$ were found to be preferable precursor materials for depositing ZnS films by CBD. In addition, $ZnSO_4$ and $Zn(CH_3COO)_2$ showed their potentiality to improve the mechanical properties of ZnS film.

ACKNOWLEDGEMENTS

The authors are grateful to L. Zhou, H. Ke, Y. Jhang, S. W. Shin, K. Deepa, G. L. Agawane, T. B. Nasr, H. Lekiket, Y. C. Lin, P. Roy, H. Haddad, Y. C. Yeh, M. Cao, T. Liu, their co-workers, and the publishers of the journals (Elsevier B. V. Netherland and American Physical Society) whose works have been reviewed here.

REFERENCES

1. J.H. Cha, S.M. Kwon, J.A. Bae, S.H. Yang, and C.W. Jeon, *J. Alloys Compd.* 708, 562 (2017).
2. K. Kim and W.N. Shafarman, *Nano Energy* 30, 488 (2016).
3. X.S. Fang, Y. Bando, G.Z. Shen, C.H. Ye, U.K. Gautam, P.M.F.J. Costa, C.Y. Zhi, C.C. Tang, and D. Golberg, *Adv. Mater.* 19, 2593 (2007).
4. E.N. Harvey, *A History of Luminescence From the Earliest Times Until 1900* (Philadelphia: American Philosophical Society, 1957).
5. A. Khare, S. Mishra, D.S. Kshatri, and S. Tiwari, *J. Electron. Mater.* 46, 687 (2017).
6. T. Sidot, *Comptes Rend. Acad. Sci.* 62, 999 (1866).
7. G. Destriau, *J. Chim. Phys.* 33, 587 (1936).
8. A. Mukherjee and S. Ghosh, *Phys. E Low-Dimens. Syst. Nanostruct.* 64, 234 (2014).
9. S. Khan, L.S.A. Carneiro, E.C. Romani, D.G. Larrudé, and R.Q. Aucelio, *J. Lumin.* 156, 16 (2014).
10. C. Shu, L. Ding, and W. Zhong, *Spectrochim Acta. Part A Mol. Biomol. Spectrosc.* 131, 195 (2014).
11. F. Chen, Y. Cao, and D. Jia, *Chem. Eng. J.* 234, 223 (2013).
12. L. Zhang, R. Dong, Z. Zhu, and S. Wang, *Sens. Actuator B Chem* 245, 112 (2017).
13. X. Dong, J. Xu, S. Shi, X. Zhang, L. Li, and S. Yin, *J. Phys. Chem. Solids* 104, 133 (2017).
14. Z. Gang, Z. Pei, N. Tongjun, L. Lin, D. Jiatao, J. Yong, J. Zhifeng, and S. Xiaosong, *Mater. Lett.* 189, 263 (2017).
15. S. Park, S. An, Y. Mun, and C. Lee, *Curr. Appl. Phys.* 14, 57 (2014).
16. S.K. Maji, A.K. Dutta, D.N. Srivastava, P. Paul, A. Mondal, and B. Adhikary, *Polyhedron* 30, 2493 (2011).
17. Y. Lun, Y. Lin, Y. Meng, and Y. Wang, *Ceram. Int.* 40, 8157 (2014).
18. C. Liu, L. Mu, J. Jia, X. Zhou, and Y. Lin, *Electrochim. Acta* 111, 179 (2013).
19. X. Ma, J. Song, and Z. Yu, *Thin Solid Films* 519, 5043 (2011).
20. T. Kryshtab, V.S. Khomchenko, J.A. Andraca-Adame, A.K. Savin, A. Kryvko, G. Juárez, and R. Peña-Sierra, *J. Lumin.* 129, 1677 (2009).
21. S.K. Mehta, Khushboo, and A. Umar, *Talanta* 85, 2411 (2011).
22. L. Wang, S. Huang, and Y. Sun, *Appl. Surf. Sci.* 270, 178 (2013).
23. S. Ummartyotin, N. Bunnak, J. Juntaro, M. Sain, and H. Manuspiya, *Solid State Sci.* 14, 299 (2012).
24. H. Labiadh, B. Sellami, A. Khazri, W. Saidani, and S. Khemais, *Opt. Mater.* 64, 179 (2017).
25. X. Fang, Y. Bando, U.K. Gautam, C. Ye, and D. Golberg, *J. Mater. Chem.* 18, 509 (2008).
26. T. Zhai, X. Fang, L. Li, Y. Bando, and D. Golberg, *Nanoscale* 2, 168 (2010).
27. X. Fang, Y. Bando, U.K. Gautam, T. Zhai, H. Zeng, X. Xu, M. Liao, and D. Golberg, *Crit. Rev. Solid State Mater. Sci.* 34, 190 (2009).
28. X. Fang, T. Zhai, U.K. Gautam, L. Li, L. Wu, Y. Bando, and D. Golberg, *Prog. Mater Sci.* 56, 175 (2011).
29. R. Kamada, T. Yagioka, S. Adachi, A. Handa, K.F. Tai, T. Kato, and H. Sugimoto, in *43rd IEEE Photovoltaic Specialists Conference*, pp. 1287–1291 (2016).
30. R. Bhattacharya and K. Ramanathan, *Sol. Energy* 77, 679 (2004).
31. J.Y. Park, R.B.V. Chalapathy, A.C. Lokhande, C.W. Hong, and J.H. Kim, *J. Alloys Compd.* 695, 2652 (2017).
32. C.P. Bjorkman, T. Torndahl, D. Abou-Ras, J. Malmstrom, J. Kessler, and L. Stolt, *J. Appl. Phys.* 100, 044506 (2006).
33. T. Nakada, M. Mizutani, Y. Hagiwara, and A. Kunioka, *Sol. Energy Mater. Sol. Cells* 67, 255 (2001).
34. M. Zuo, S. Tan, G.P. Li, and S.Y. Zhang, *Sci. China Phys. Mech. Astron.* 55, 219 (2012).
35. J.J. Ho, W.T. Hsu, C.C. Chiang, S.Y. Tsai, S.S. Wang, C.K. Lin, C.C. Chou, C.H. Yeh, and K.L. Wang, *Mater. Sci. Semicond. Process.* 59, 29 (2017).
36. A. Khare, *J. Optoelectron. Adv. Mater.* 11, 1805 (2009).
37. X.J. Zhang, M.W. Zhao, S.S. Yan, T. He, W.F. Li, X.H. Lin, Z.X. Xi, Z.H. Wang, X.D. Liu, and Y.Y. Xia, *Nanotechnology* 19, 305708 (2008).
38. C.Y. Yeh, Z.W. Lu, S. Froyen, and A. Zunger, *Phys. Rev. B* 46, 10086 (1992).
39. T.K. Tran, W. Park, W. Tong, M.M. Kyi, B.K. Wagner, and C.J. Summers, *J. Appl. Phys.* 81, 2803 (1997).
40. H. Chen, D. Shi, J. Qi, J. Jia, and B. Wang, *Phys. Lett. A* 373, 371 (2009).
41. F. Ghribi, L.E. Mir, K. Omri, and K. Djessas, *Optik* 127, 3688 (2016).
42. T.K. Pathak, V. Kumar, L.P. Purohit, H.C. Swart, and R.E. Kroon, *Physica E* 84, 530 (2016).
43. K. Ghezali, L. Mentar, B.R. Boudine, and A. Azizi, *J. Electroanal. Chem.* 794, 212 (2017).
44. K.L. Chopra, R.C. Kainthla, D.K. Pandya, and A.P. Thakur, *Phys. Thin Films* 12, 201 (1982).
45. C.D. Lokhande, *Mater. Chem. Phys.* 28, 145 (1991).
46. R.S. Mane and C.D. Lokhande, *Mater. Chem. Phys.* 65, 1 (2000).
47. P.K. Nair, M.T.S. Nair, A. Femandez, and M. Ocampo, *J. Phys. D Appl. Phys.* 22, 829 (1989).
48. B.M. Basol and V.K. Kapur, *IEEE Trans. Electron Dev.* 37, 418 (1990).
49. P. Jackson, D. Hariskos, E. Lotter, S. Paetel, R. Wuerz, R. Menner, W. Wischmann, and M. Powalla, *Prog. Photovolt. Res. Appl.* 19, 894 (2011).
50. P. O'Brien and J. McAleese, *J. Mater. Chem.* 8, 2309 (1998).
51. J.M. Doña and J. Herrero, *J. Electrochem. Soc.* 144, 4081 (1997).
52. P.K. Nair, P. Parmananda, and M.T.S. Nair, *J. Cryst. Growth* 206, 68 (1999).
53. M. Kostoglou, N. Andritsos, and A.J. Karabelas, *Thin Solid Films* 387, 115 (2001).
54. L. Zhou, N. Tang, and S. Wu, *Surf. Coat. Technol.* 228, S146 (2013).
55. H. Ke, S. Duo, T. Liu, Q. Sun, C. Ruan, X. Fei, J. Tan, and S. Zhan, *Mater. Sci. Semicond. Process.* 18, 28 (2014).
56. B.Z. Dong, G.J. Fang, J.F. Wang, W.J. Guan, and X.Z. Zhao, *J. Appl. Phys.* 101, 033713 (2007).
57. G. Liang, P. Fan, C. Chen, J. Luo, J. Zhao, and D. Zhang, *J. Mater. Sci. Mater. Electron.* 26, 2230 (2015).
58. J.M. Dona and J. Herrero, *J. Electrochem. Soc.* 141, 205 (1994).
59. C. Hubert, N. Naghavi, O. Roussel, A. Etcheberry, D. Hariskos, R. Menner, M. Powalla, O. Kerrec, and D. Lincot, *Prog. Photovolt. Res. Appl.* 17, 470 (2009).
60. Y. Zhang, X.Y. Dang, J. Jin, T. Yu, B.Z. Li, Q. He, F.Y. Li, and Y. Sun, *Appl. Surf. Sci.* 256, 6871 (2010).
61. F. Gode, C. Gumus, and M. Zor, *J. Cryst. Growth* 299, 136 (2007).
62. S.W. Shin, G.L. Agawane, M.G. Gang, A.V. Moholkar, J. Moon, J.H. Kim, and J.Y. Lee, *J. Alloys Compd.* 526, 25 (2012).
63. G.L. Agawane, S.W. Shin, A.V. Moholkar, K.V. Gurav, J.H. Yun, J.Y. Lee, and J.H. Kim, *J. Alloys Compd.* 535, 53 (2012).
64. K. Deepa, K.C. Preetha, K.V. Murali, A.C. Dhanya, A.J. Ragina, and T.L. Remadevi, *Optik* 125, 5727 (2014).
65. P.U. Londhe, A.B. Rohom, G.R. Bhand, S. Jadhav, M.G. Lakhe, and N.B. Chaure, *J. Mater. Sci.: Mater. Electron.* 28, 5207 (2017).
66. T.B. Nasr, N. Kamoun, M. Kanzari, and R. Bennaceur, *Thin Solid Films* 500, 4 (2006).
67. P.A. Luque, A. Castro-Beltran, A.R. Vilchis-Nestr, M.A. Quevedo-Lopez, and A. Olivas, *Mater. Lett.* 140, 148 (2015).
68. H. Lekiket and M.S. Aida, *Mater. Sci. Semicond. Process.* 16, 1753 (2013).
69. K. Ahn, J.H. Jeon, S.Y. Jeong, J.M. Kim, H.S. Ahn, J.P. Kim, E.D. Jeong, and C.R. Cho, *Curr. Appl. Phys.* 12, 1465 (2012).
70. Z.Q. Li, J.H. Shi, Q.Q. Liu, Z.A. Wang, Z. Sun, and S.M. Huang, *Appl. Surf. Sci.* 257, 122 (2010).

71. Y.C. Lin, Y.T. Chao, and P.C. Yao, *Appl. Surf. Sci.* 307, 724 (2014).
72. P. Roy, J.R. Ota, and S.K. Srivastava, *Thin Solid Films* 515, 1912 (2006).
73. Q. Liu, M. Guobing, and A. Jianping, *Appl. Surf. Sci.* 254, 5711 (2008).
74. Y. Kavanagh and D.C. Cameron, *Thin Solid Films* 398, 24 (2001).
75. Y.T. Nien, S.C. Tsai, and I.G. Chen, *J. Cryst. Growth* 287, 128 (2006).
76. S.W. Shin, S.R. Kang, J.H. Yun, A.V. Moholkar, J. Moon, J.Y. Lee, and J.H. Kim, *Sol. Energy Mater. Sol. Cells* 95, 856 (2011).
77. M. Cao, B.L. Zhang, L. Li, J. Huang, S.R. Zhao, H. Cao, J.C. Jiang, Y. Sun, and Y. Shen, *Mater. Res. Bull.* 48, 357 (2013).
78. S. Tec-Yam, J. Rojas, V. Rejón, and A.I. Oliva, *Mater. Chem. Phys.* 136, 386 (2012).
79. P.A. Luque, M.A. Quevedo-Lopez, and A. Olivas, *Mater. Lett.* 106, 49 (2013).
80. F.G. Hone, F.K. Ampong, T. Abza, I. Nkrumah, M. Paal, R.K. Nkum, and F. Boakye, *Mater. Lett.* 155, 58 (2015).
81. H. Haddad, A. Chelouche, D. Talantikite, H. Merzouk, F. Boudjouan, and D. Djouadi, *Thin Solid Films* 589, 451 (2015).
82. Y.G. Wang, S.P. Lau, X.H. Zhang, H.H. Hng, H.W. Lee, S.F. Yu, and B.K. Tay, *J. Cryst. Growth* 259, 335 (2003).
83. X. Zhang, H. Song, L. Yu, T. Wang, X. Ren, X. Kong, Y. Xie, and X. Wang, *J. Lumin.* 118, 251 (2006).
84. T. Liu, H. Ke, H. Zhang, S. Duo, Q. Sun, X. Fei, G. Zhou, H. Liu, and L. Fan, *Mater. Sci. Semicond. Process.* 26, 301 (2014).
85. T. Liu, Y. Li, H. Ke, Y. Qian, S. Duo, Y. Hong, and X. Sun, *J. Mater. Sci. Technol.* 32, 207 (2016).
86. T. Kobayashi, T. Kumazawa, Z.J.L. Kao, and T. Nakada, *Sol. Energy Mater. Sol. Cells* 123, 197 (2014).
87. A.T. Salih, A.A. Najim, M.A.H. Muhi, and K.R. Gbashi, *Opt. Commun.* 388, 84 (2017).
88. R. Sahraei and S. Darafarin, *J. Lumin.* 149, 170 (2014).
89. A. Jrad, T.B. Nasr, and N. Turki-Kamoun, *Opt. Mater.* 50, 128 (2015).
90. S. Darafarin, R. Sahraei, and A. Daneshfar, *J. Alloys Compd.* 658, 780 (2016).
91. P. Babu, M.R.V. Reddy, S. Kondaiah, K.T.R. Reddy, and P. Chinho, *Optik* 130, 608 (2017).
92. T.B. Nasr, N. Kamoun, and C. Guasch, *Appl. Surf. Sci.* 254, 5039 (2008).
93. A. Wei, J. Liu, M. Zhuang, and Y. Zhao, *Mater. Sci. Semicond. Process.* 16, 1478 (2013).
94. M.H. Doha, M.J. Alam, J. Rabeya, K.A.M.H. Siddiquee, S. Hussain, O. Islam, M.A. Gafur, S. Islam, N. Khatun, and S.H. Sarkar, *Optik* 126, 5194 (2015).
95. S.W. Shin, S.R. Kang, K.V. Gurav, J.H. Yun, J. Moon, J.Y. Lee, and J.H. Kim, *Sol. Energy* 85, 2903 (2011).
96. C.A. Rodríguez, M.G. Sandoval-Paz, G. Cabello, M. Flores, H. Fernández, and C. Carrasco, *Mater. Res. Bull.* 60, 313 (2014).
97. F. Long, W.M. Wanga, Z. Cui, L. Fan, Z. Zou, and T. Jia, *Chem. Phys. Lett.* 462, 84 (2008).